

Electronic Supplementary Information

Bispidine as a promising scaffold for designing molecular machines

Hanuman Singh,^a Akshay Chenna,^b Upanshu Gangwar,^a Souvik Dutta,^a Narayanan D. Kurur,^a Gaurav Goel,^b V. Haridas*^a

^aDepartment of Chemistry, Indian Institute of Technology Delhi, Hauz Khas, New Delhi-110016, India

^bDepartment of Chemical Engineering, Indian Institute of Technology Delhi, Hauz Khas, New Delhi-110016, India.

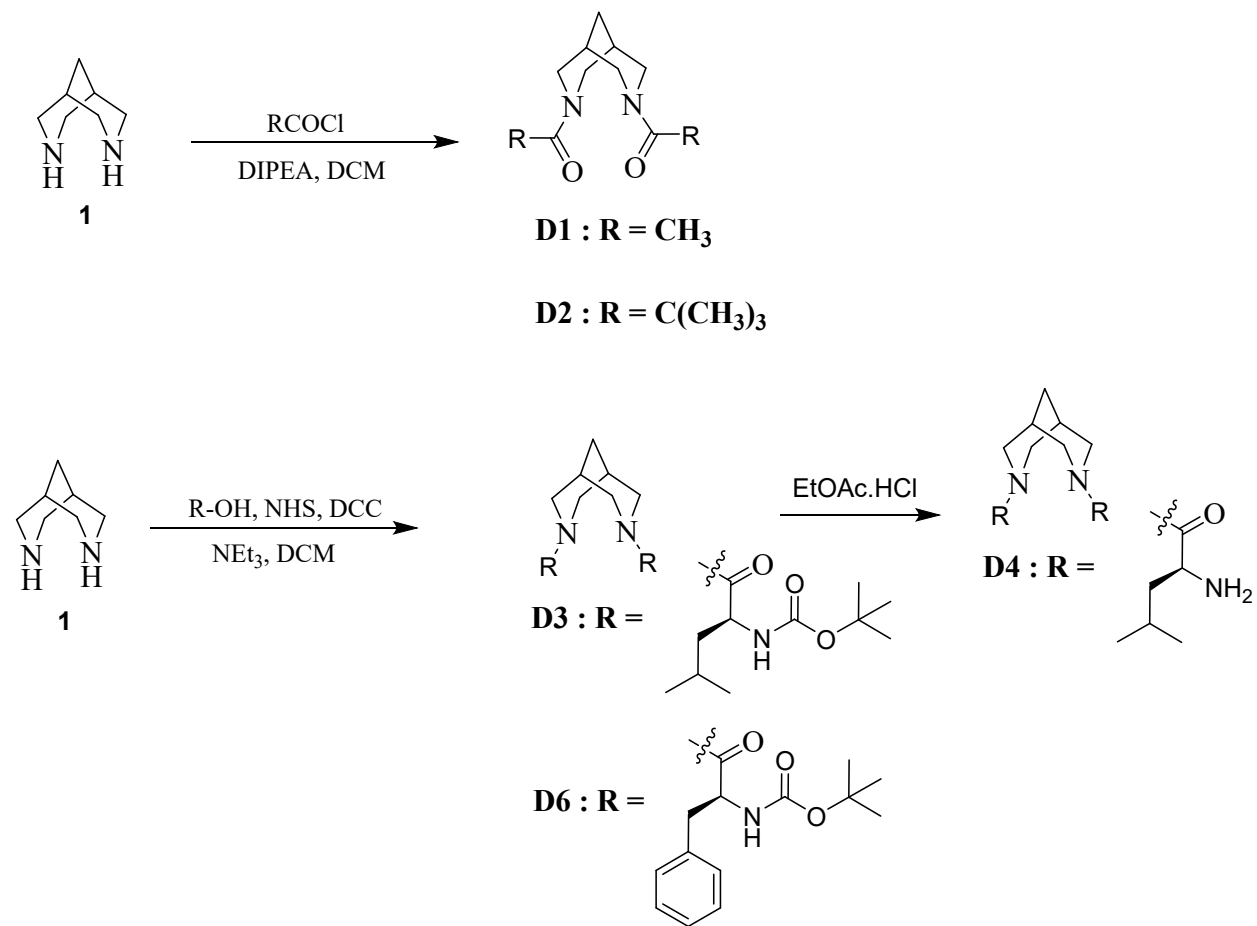
E-mail: haridasv@chemistry.iitd.ac.in

General Experimental Section	S2
Synthetic schemes	S3
Preparation of compounds	S4-S8
Crystal data of D2	S9
¹ H NMR spectra of D1 in different solvents	S10
HSQC spectrum of D1 in CDCl ₃	S11
Temperature-dependent ¹³ C NMR of D2	S12
COSY spectrum of D2 298 K	S13
¹ H NMR spectra of D1 and D2 in presence of LaCl ₃	S14
¹ H NMR titration study of D3	S15
¹ H NMR spectra of D3 in different solvents	S16
¹ H NMR spectra of D3 at different temperature	S17-S18
TOCSY spectra of D3 and D5	S19
Dynamic NMR studies on D5	S20-S25
Computational modelling	S26-S37
NMR and Mass spectral data of all synthesized compounds	S38-S57
References	S58

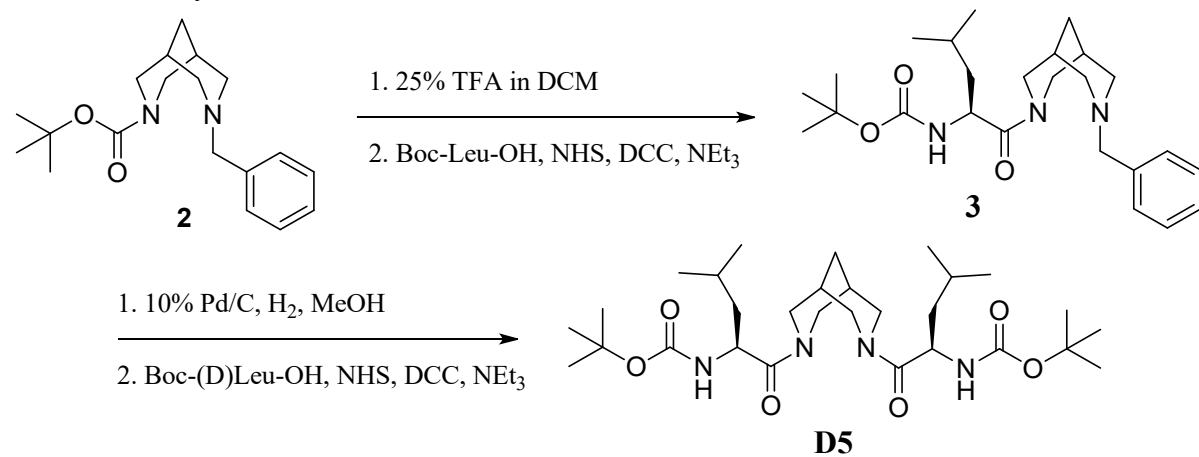
Experimental method

Reagents were purchased from Sigma-Aldrich, USA or Alfa Aesar (India). All the chemical reactions were monitored by thin-layer chromatography (TLC) using silica gel plates (Merck USA). Compounds were purified by silica gel (100–200 and 60-120 mesh) column chromatography. The solvents used were dried by standard methods. Infrared spectra were recorded on a Perkin Elmer spectrum IR, version 10.6.0 using KBr pellets. Characterizations were done by ^1H NMR, ^{13}C NMR, IR, and high-resolution mass spectrometry (HRMS). ^1H and ^{13}C NMR spectra were recorded on Bruker-DPX- 300MHz and Bruker 500 MHz spectrometers, and the chemical shifts were reported relative to tetramethylsilane as the reference. Mass spectra (HRMS) were recorded on a Bruker MicrO-TOF-QII model using ESI technique. Melting points were recorded by a Fisher scientific melting point apparatus. X-ray diffraction analysis was carried out on a BRUKER AXS SMARTAPEX diffractometer with a CCD area detector (Mo $K\alpha = 0.71073\text{\AA}$, monochromator: S3 graphite). Structure solution, refinement, and data output were carried out with the ShelXTL program.

Synthetic schemes



Scheme S1: Synthesis of D1-D4, and D6.



Scheme S2: Synthesis of D5.

Sch

Synthesis of D1:

To a well-stirred ice-cooled solution of **1** (0.410 g, 3.249 mmol) in dichloromethane (DCM) was added N,N-diisopropylethylamine (DIPEA) (1.245 mL, 7.148 mmol) and acetyl chloride (0.462 mL, 6.498 mmol) and stirred for 8 h. After the completion of the reaction, the mixture was washed with 0.2N H₂SO₄, saturated aq. NaHCO₃ and water. The organic part was collected and dried over anhyd. Na₂SO₄ and evaporated under vacuum to obtain the crude product, which was purified by silica gel column chromatography (Ethyl acetate/Hexane) to obtain 0.608 g of **D1** as solid.

Yield= 89 %, Mp: 138-140 °C;

¹H NMR (CD₃OD, 500 MHz): 1.85 (br s, 4H), 1.94 (s, 6H), 1.97 (minor), 2.78 (d, *J* = 13.5 Hz, 2H), 3.29 (d, *J* = 13.5 Hz, 2H), 3.93 (d, *J* = 13.5 Hz, 2H), 3.98 (d, *J* = 13 Hz, minor), 4.42 (d, *J* = 13.5 Hz, minor), 4.64 (d, *J* = 13.5 Hz, 2H).

¹H NMR (DMSO-*d*₆, 500 MHz): 1.80 (m, 4H), 1.86 (s, 6H), 1.95 (minor), 2.69 (minor), 2.71 (d, *J* = 13.5 Hz, 2H), 3.25 (d, *J* = 13.5 Hz, 2H), 3.85 (d, *J* = 13 Hz, 2H), 3.97 (d, *J* = 13 Hz, minor), 4.31 (d, *J* = 13.5 Hz, minor), 4.60 (d, *J* = 13 Hz, 2H).

¹H NMR (CDCl₃, 500 MHz): 1.91 (br s, 2H), 1.94 (br s, 2H), 2.02 (s, 6H), 2.82 (d, *J* = 13.5 Hz, 2H), 3.33 (d, *J* = 13 Hz, 2H), 3.95 (d, *J* = 13 Hz, 2H), 4.83 (d, *J* = 13.5 Hz, 2H); ¹³C NMR (CDCl₃, 125 MHz): δ 21.6, 27.8, 31.7, 45.8, 50.8, 170.2; IR (KBr): 2927, 2867, 2203, 1682, 1615, 1464, 1448, 1258, 1026 cm⁻¹; HRMS: calcd for C₁₁H₁₈N₂NaO₂ m/z 233.1260, found m/z 233.1257.

Synthesis of D2:

To a well-stirred ice-cooled solution of **1** (0.410 g, 3.249 mmol) in DCM containing DIPEA (1.245 mL, 7.148 mmol) was added pivaloylchloride (0.799 mL, 6.498 mmol) and stirred for 8 h. After

the completion of the reaction, the mixture was washed with 0.2N H₂SO₄, saturated aq. NaHCO₃ and water. The organic part was collected and dried over anhyd. Na₂SO₄ and evaporated under vacuum to obtain the crude product, and was purified by silica gel column chromatography (Ethyl acetate/Hexane) to obtain 0.832 g of **D2** as solid.

Yield: 87 %, Mp: 168-170 °C;

¹H NMR (CDCl₃, 500 MHz): δ 1.23 (s, 18H), 1.84 (s, 2H), 2.03 (s, 2H), 3.10 (br s, 4H), 4.48 (br s, 4H); ¹³C NMR (CDCl₃, 125 MHz): δ 28.5, 28.6, 31.6, 38.9, 49.4, 176.9; IR (KBr): 2964, 2922, 2843, 1618, 1473, 1415, 1361, 1189 cm⁻¹; HRMS: calcd for C₁₇H₃₀N₂NaO₂ m/z 317.2199, found m/z 317.2200.

Synthesis of **D3**:

To a well stirred solution of tert-butyloxy carbonyl (Boc) protected leucine (1.503 g, 6.498 mmol) in DCM was added N-hydroxysuccinimide (NHS) (0.897 g, 7.798 mmol), N,N'-dicyclohexylcarbodiimide (DCC) (1.609 g, 7.798 mmol) followed by **1** (0.410 g, 3.249 mmol), and triethylamine (NEt₃) (1.09 ml, 7.798mmol). The resultant solution was stirred for 24 h at room temperature. After the completion of the reaction, the mixture was evaporated and re-dissolved in ethyl acetate and filtered. The filtrate was washed with 0.2N H₂SO₄, saturated aq. NaHCO₃ and water. The organic part was collected and dried over anhyd. Na₂SO₄ and evaporated under vacuum to obtain the crude product, and was purified by silica gel column chromatography (Ethyl acetate/Hexane) to obtain 1.525 g of **D3** as solid.

Yield: 85 %

¹H NMR (CDCl₃, 500 MHz): δ 0.88 (d, *J* = 6.5 Hz, minor), 0.93 (d, *J* = 7 Hz, 6H), 0.95 (d, *J* = 6.5 Hz, minor), 1.02 (d, *J* = 6.5 Hz, 6H), 1.16 (m, minor), 1.28 (m, 4H), 1.40 (s, 18H), 1.50 (s, minor),

1.63 (m, minor), 1.69 (m, 2H), 1.88 (s, 2H), 1.90 (s, minor), 1.99 (s, minor), 2.120 (s, 2H), 2.84 (d, $J = 13.5$ Hz, minor), 3.00 (d, $J = 14$ Hz, 2H), 3.26 (d, $J = 13$ Hz, minor), 3.41 (d, $J = 12.5$ Hz, 2H), 3.81 (d, $J = 13$ Hz, 2H), 4.06 (d, $J = 13$ Hz, minor), 4.46 (m, 4H), 4.57 (m, minor), 4.68 (d, $J = 14$ Hz, 1H), 5.22 (d, $J = 9$ Hz, 2H), 5.59 (d, $J = 8$ Hz, minor); ^{13}C NMR (CDCl_3 , 75 MHz): δ 21.4, 22.2, 23.4, 23.5, 24.4, 24.7, 27.4, 28.3, 28.5, 30.0, 43.0, 43.6, 45.9, 46.8, 48.5, 48.7, 49.6, 49.8, 79.3, 155.7, 171.5, 173.0; IR (KBr): 3403, 3326, 2961, 2931, 2868, 1711, 1658, 1628, 1531, 1452, 1436, 1366, 1244, 1172 cm^{-1} ; HRMS: calcd for $\text{C}_{29}\text{H}_{52}\text{N}_4\text{NaO}_6$ m/z 575.3785, found m/z 575.3780.

Synthesis of **D4**:

To a well stirred and ice cooled solution of **D3** (0.100 g, 0.181 mmol) in DCM (10 mL) was added EtOAc.HCl and the reaction mixture was stirred for 4 h at room temperature. The reaction mixture was evaporated and washed with pentane thrice to obtain 0.064 g of **D4** as a colorless liquid.

^1H NMR ($\text{DMSO}-d_6$, 500 MHz): 0.84 (d, $J = 6.5$ Hz, 6H), 0.89 (d, $J = 6.5$ Hz, 6H), 0.94 (d, $J = 6.5$ Hz, 6H), 0.96 (d, $J = 6.5$ Hz, 6H), 1.14 (m, 2H), 1.49 (m, 6H), 1.81 (m, 8H), 2.00 (br s, 2H), 2.15 (br s, 2H), 2.84 (d, $J = 13$ Hz, 2H), 2.92 (d, $J = 13$ Hz, 2H), 3.32 (d, $J = 12.5$ Hz, 2H), 3.38 (d, $J = 12.5$ Hz, 2H), 3.55 (d, $J = 13.5$ Hz, 2H), 3.82 (d, $J = 12.5$ Hz, 2H), 4.08 (br m, 2H), 4.20 (br m, 2H), 4.27 (d, $J = 13.5$ Hz, 2H), 4.51 (d, $J = 13.5$ Hz, 2H), 8.16 (br s, 4H), 8.29 (br s, 4H); ^{13}C NMR ($\text{DMSO}-d_6$, 125 MHz): δ 21.6, 22.1, 23.4, 23.7, 23.8, 24.0, 27.0, 28.1, 29.3, 30.5, 39.3, 41.1, 46.0, 47.2, 48.5, 49.1, 50.0, 50.2, 168.5, 169.7; IR (KBr): 3435, 2928, 1642, 1465, 1021 cm^{-1} ; HRMS: calcd for $\text{C}_{19}\text{H}_{37}\text{N}_4\text{O}_2$ m/z 353.2917, found m/z 353.2909.

Synthesis of **D5**:

To a well-stirred solution of **3**¹ (0.700g, 1.629 mmol) in methanol (15mL) was added palladium-charcoal catalyst (0.070g) and the reaction mixture was stirred for 4 h at room temperature. The reaction mixture was filtered, evaporated and used as such for further reaction.

The obtained amine was added to the DCM solution containing Boc-protected D-leucine (0.438 g, 1.896 mmol), NHS (0.262 g, 2.275 mmol), DCC (0.469 g, 2.275 mmol) and NEt₃ (0.317 mL, 2.275 mmol). The reaction solution was stirred for 24 h at room temperature. After completion of the reaction, the mixture was evaporated and re-dissolved in ethyl acetate and filtered. The filtrate was washed with 0.2N H₂SO₄, saturated aq. NaHCO₃ and water. The organic part was collected and dried over anhyd. Na₂SO₄ and evaporated under vacuum to obtain the crude product, and was purified by silica gel column chromatography (Ethyl acetate/Hexane) to obtain 0.755 g of **D5** as solid.

Yield: 84 %, Mp: 88-90 °C;

¹H NMR (CDCl₃, 500 MHz): δ 0.88 (d, *J* = 6.5 Hz, 6H), 0.97 (d, *J* = 6.5 Hz, 6H), 1.02 (d, *J* = 6.5 Hz, 6H), 1.29 (m, 6H), 1.35 (m, 6H), 1.41 (s, 18H), 1.46 (s, 18H), 1.67 (m, 4H), 1.89 (br s, 4H), 2.10 (br s, 4H), 2.88 (d, *J* = 13.5 Hz, 2H), 3.00 (d, *J* = 14 Hz, 2H), 3.29 (d, *J* = 12.5 Hz, 2H), 3.41 (d, *J* = 13 Hz, 2H), 3.88 (d, *J* = 13 Hz, 2H), 4.02 (d, *J* = 12.5 Hz, 2H), 4.48 (d, *J* = 14 Hz, 2H), 4.56 (m, 2H), 4.66 (m, 4H), 5.15 (d, *J* = 9.5 Hz, 2H), 5.37 (d, *J* = 8.5 Hz, 2H); ¹³C NMR (CDCl₃, 125 MHz): δ 21.5, 22.3, 23.4, 23.6, 24.4, 24.7, 27.8, 28.3, 28.4, 30.6, 42.6, 42.8, 46.3, 46.8, 48.4, 48.5, 49.4, 50.0, 79.3, 155.0, 155.7, 171.5, 173.2; IR (KBr): 3412, 3352, 2957, 2870, 1727, 1694, 1638, 1514, 1452, 1366, 1255, 1175 cm⁻¹; HRMS: calcd for C₂₉H₅₂N₄NaO₆ m/z 575.3779, found m/z 575.3787.

Synthesis of **D6**:

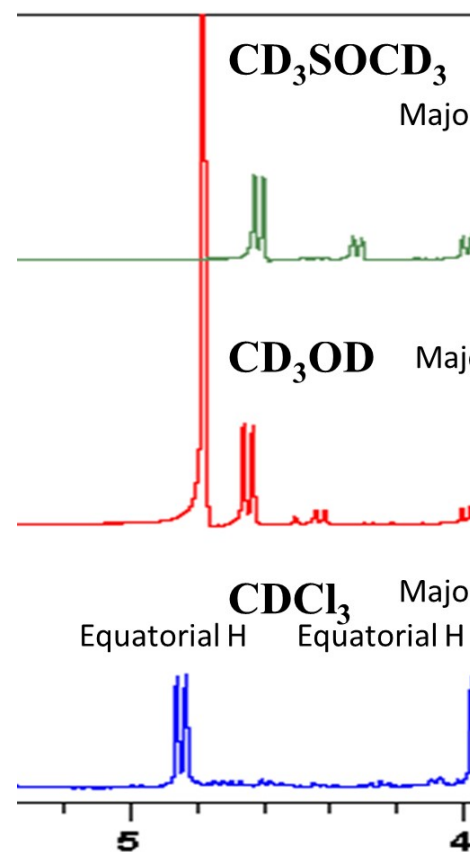
To a well stirred solution of Boc-protected phenylalanine (1.724 g, 6.498 mmol) in DCM was added NHS (0.897 g, 7.798 mmol), DCC (1.609 g, 7.798 mmol) followed by **1** (0.410 g, 3.249 mmol), and NEt₃ (0.63 ml, 4.548 mmol). After the completion of the reaction, the mixture was evaporated and re-dissolved in ethyl acetate and filtered. The filtrate was washed with 0.2N H₂SO₄, saturated aq. NaHCO₃ and water. The organic part was collected and dried over anhyd. Na₂SO₄ and evaporated under vacuum to obtain the crude product, and was purified by silica gel column chromatography (Ethyl acetate/Hexane) to obtain 1.674 g **D6** as solid.

Yield: 83 %, Mp: 218-220 °C;

¹H NMR (CDCl₃, 300 MHz): δ 1.27 (m, 4H), 1.53 (s, 18H), 2.00 (d, *J* = 12.9 Hz, 2H), 2.45 (d, *J* = 13.2 Hz, 2H), 2.82 (d, *J* = 9.9 Hz, 2H), 3.00 (d, *J* = 12.3 Hz, 2H), 3.57 (d, *J* = 12.9 Hz, 2H), 4.57 (d, *J* = 13.2 Hz, 2H), 4.77 (s, 2H), 5.75 (d, *J* = 6.6 Hz, 2H), 7.21 (m, 10H); ¹³C NMR (CDCl₃, 75 MHz): δ 28.0, 28.7, 31.7, 41.4, 45.4, 49.6, 51.3, 79.6, 126.6, 128.1, 129.6, 136.9, 155.2, 170.1; IR (KBr): 3433, 3330, 2927, 1714, 1629, 1520, 1458, 1268, 1172 cm⁻¹; HRMS: calcd for C₃₅H₄₈N₄NaO₆ m/z 643.3472, found m/z 643.3469.

Table S1: Crystal data and structure refinement for **D2** CCDC 2259004.

Identification code	D2
Empirical formula	C ₁₇ N ₂ O ₂ H ₃₀
Formula weight	294.43
Temperature/K	299(2)
Crystal system	orthorhombic
Space group	Fdd2
a/Å	17.3542(7)
b/Å	22.6322(8)
c/Å	8.8875(4)
α/°	90
β/°	90
γ/°	90
Volume/Å ³	3490.7(2)
Z	8
ρ _{calc} /g/cm ³	1.120
μ/mm ⁻¹	0.073
F(000)	1296.0
Crystal size/mm ³	0.2 × 0.18 × 0.1
Radiation	MoKα (λ = 0.71073)
2θ range for data collection/°	5.456 to 50.114
Index ranges	-20 ≤ h ≤ 20, -26 ≤ k ≤ 26, -10 ≤ l ≤ 10
Reflections collected	18866
Independent reflections	1548 [R _{int} = 0.0365, R _{sigma} = 0.0161]
Data/restraints/parameters	1548/1/99
Goodness-of-fit on F ²	1.046
Final R indexes [I ≥ 2σ (I)]	R ₁ = 0.0341, wR ₂ = 0.0850
Final R indexes [all data]	R ₁ = 0.0401, wR ₂ = 0.0904
Largest diff. peak/hole / e Å ⁻³	0.07/-0.10
Flack parameter	-0.3(4)

**Figure S1:** ¹H NMR of **D1** in different solvents shows a different ratio of minor to major forms.

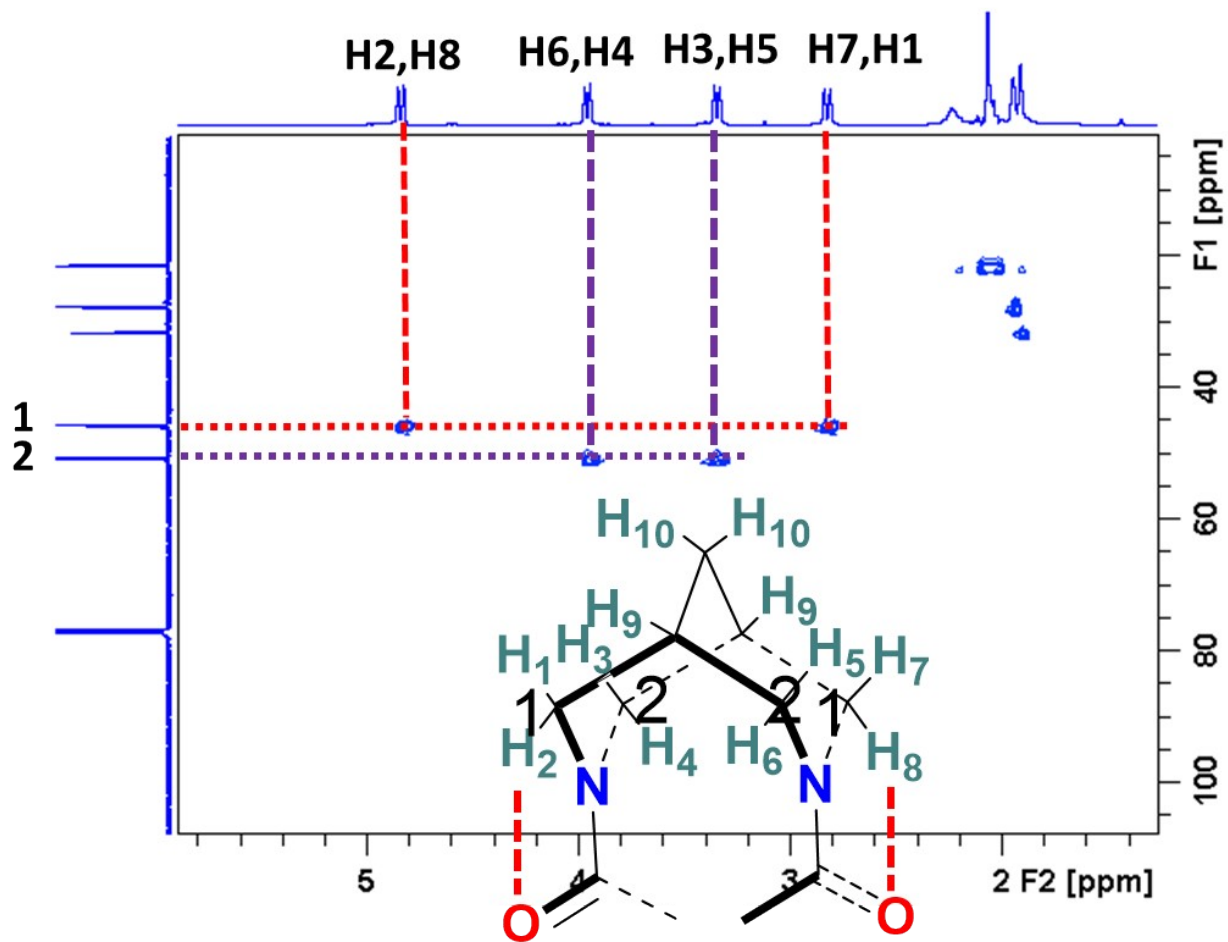


Figure S2: HSQC spectrum of **D1** in CDCl_3 showed the correlations among the protons and their respective carbons.

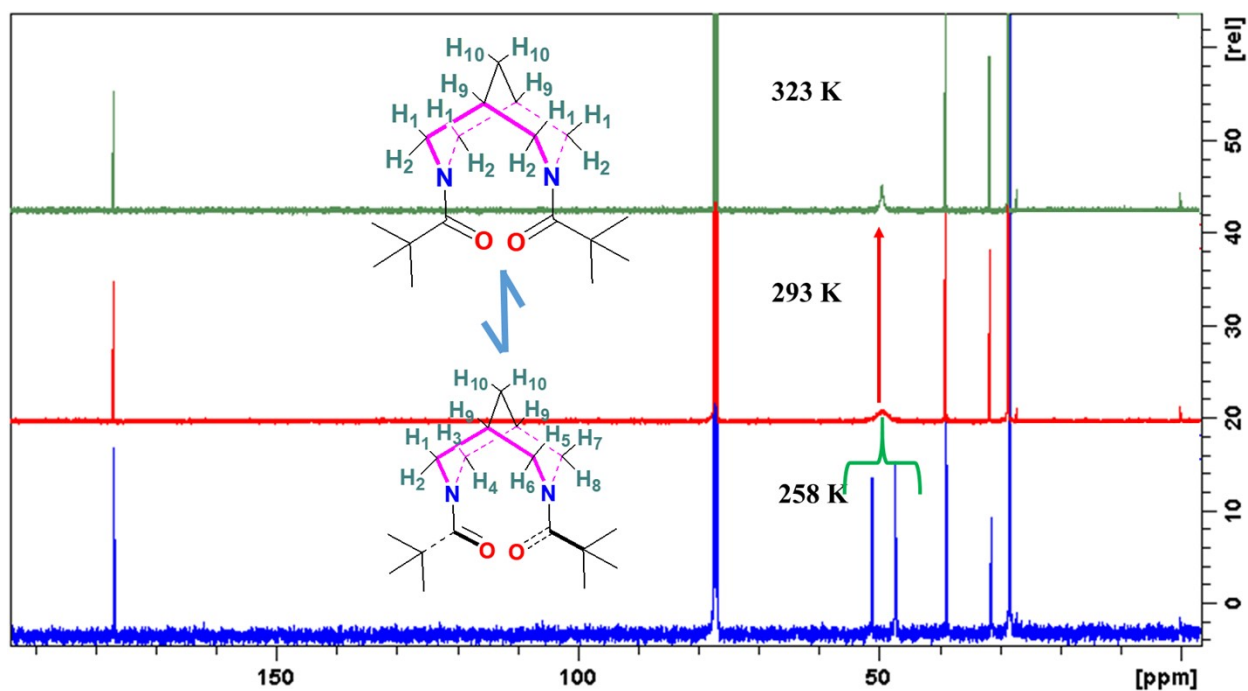


Figure S3: Temperature-dependent ^{13}C NMR of **D2** showed one signal for all methylene carbons of bispidine at room temperature and split into two signals at lower temperature.

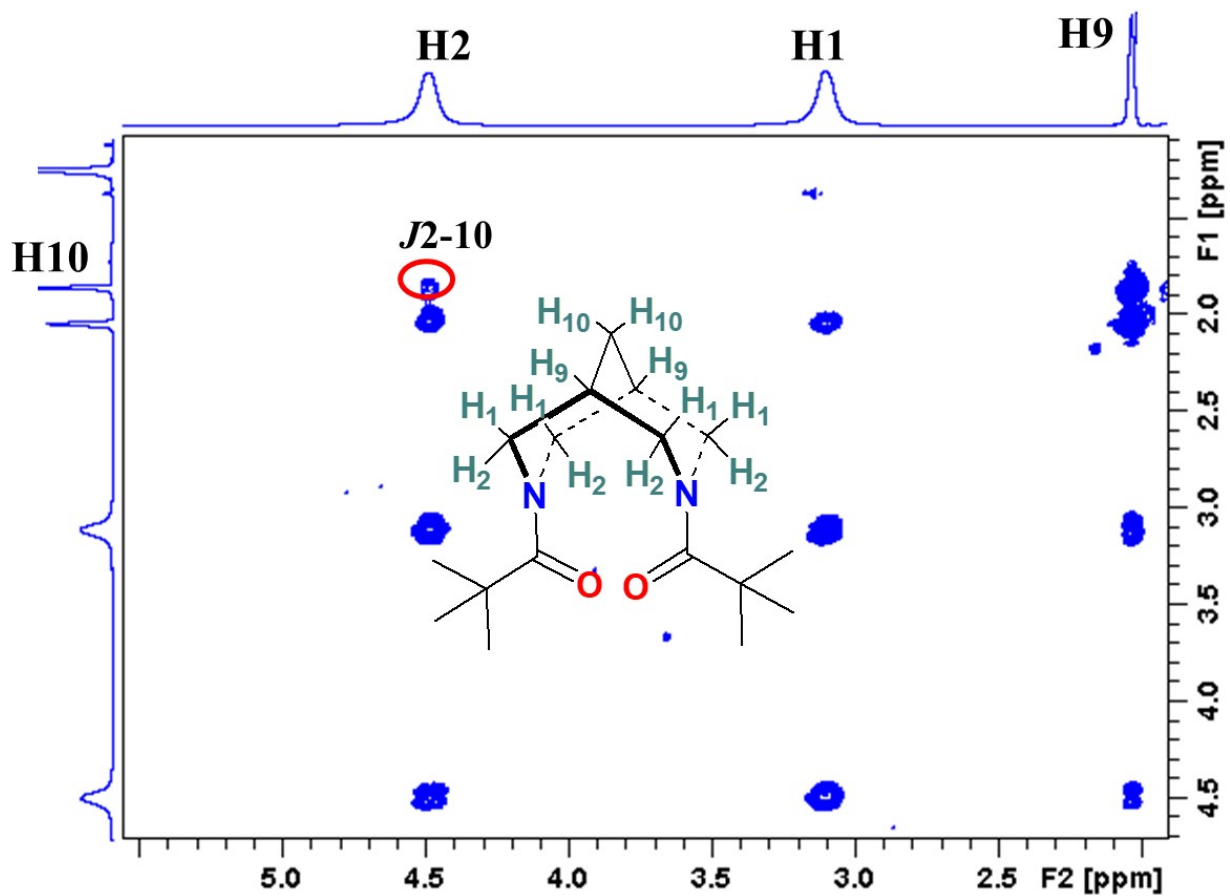


Figure S4: The COSY spectrum of **D2** 298 K. The red circles show 4J long-range coupling between the equatorial protons and bridging CH_2 (W-coupling).

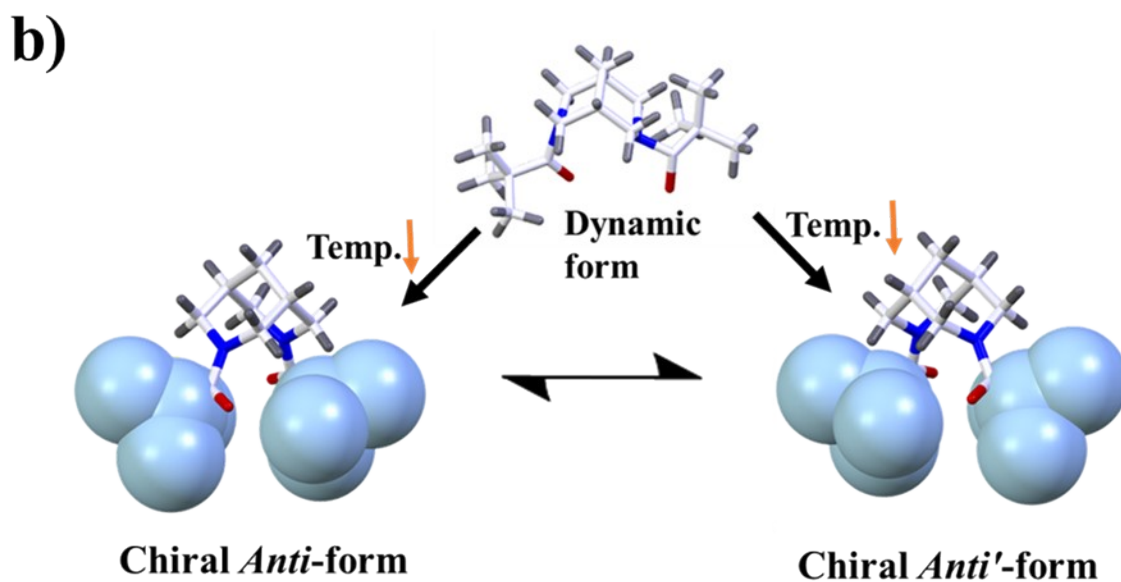
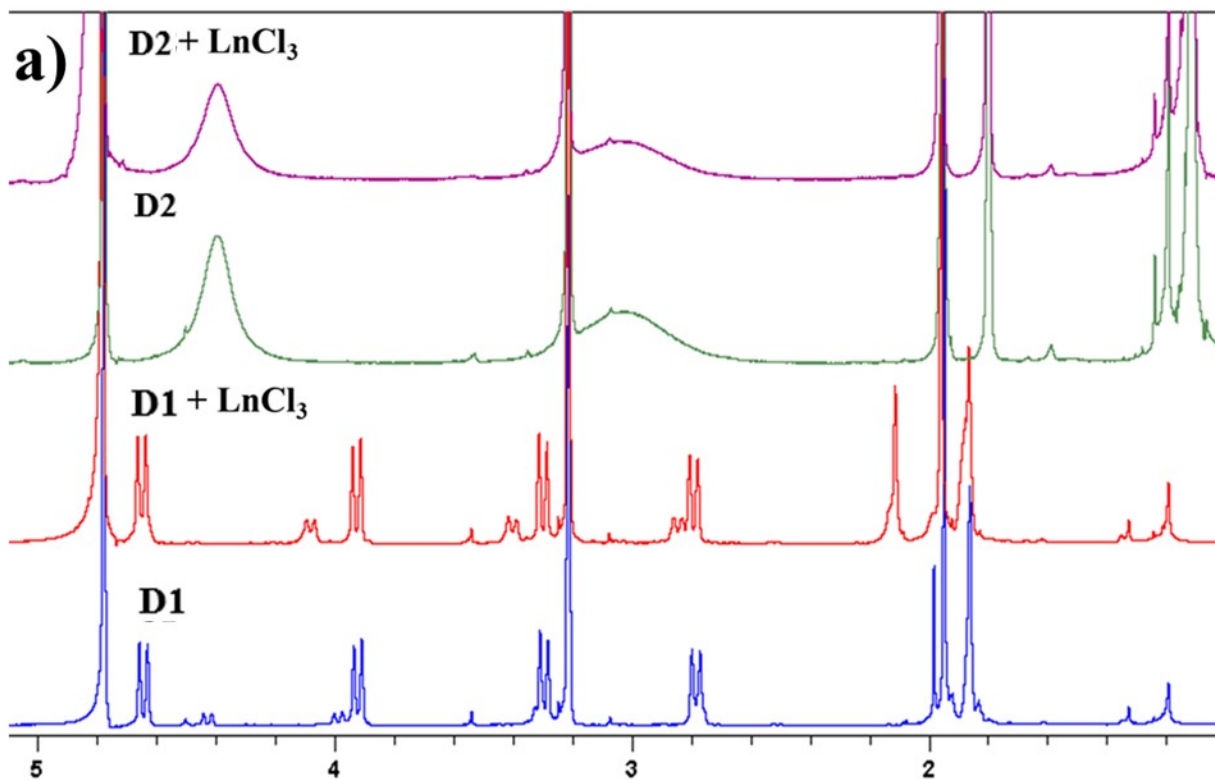


Figure S5: a) ^1H NMR spectra of **D1** shows an increased ratio of *syn* form on the addition of LaCl_3 , while there was no change in the NMR spectra for **D2**, indicating that *syn* form is unstable in **D2**. b) The possible pathway of switching of highly dynamic form (average out structure) to two chiral interconvertible *anti*-forms on decrease of temperature.

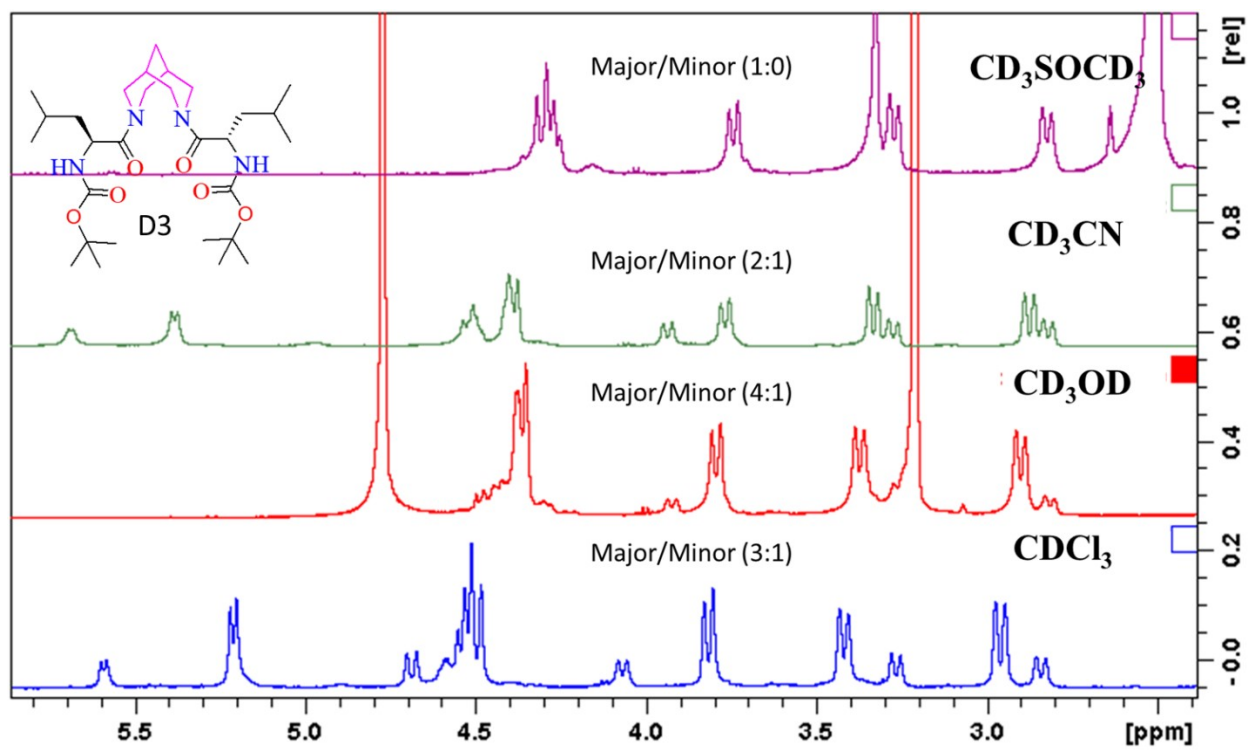


Figure S6: ¹H NMR of D3 in different solvents shows a different ratio of minor to major forms.

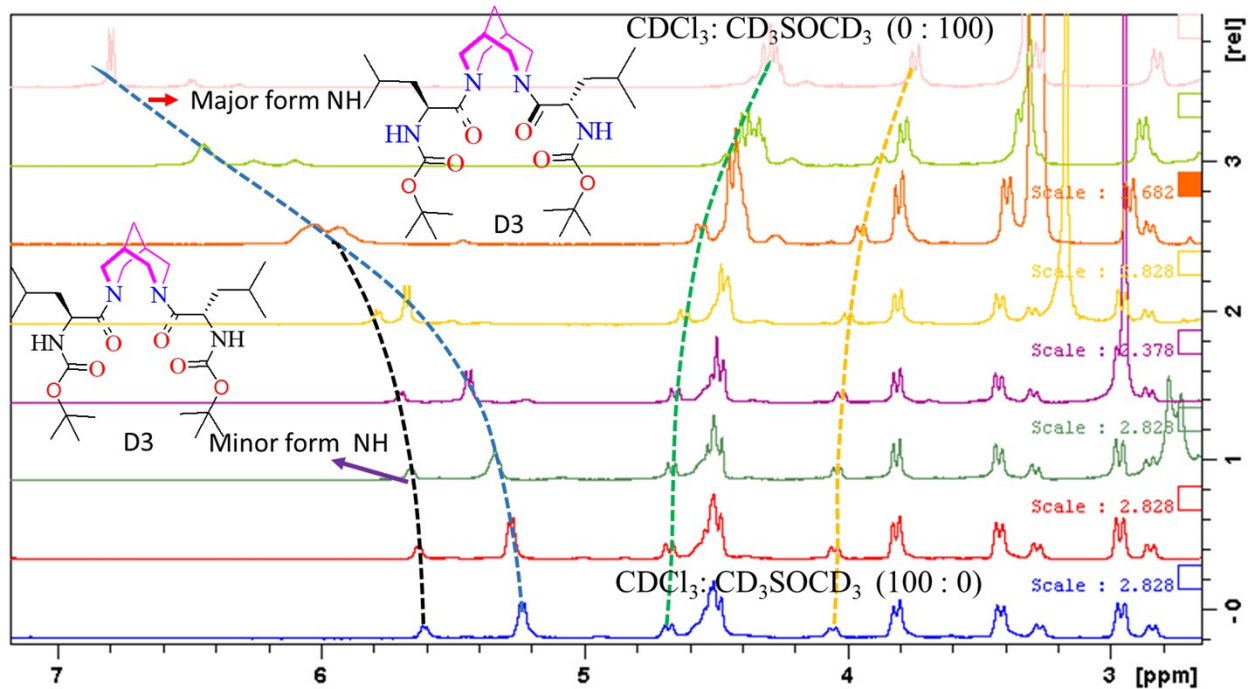


Figure S7: ^1H NMR titration study of **D3** in CDCl_3 with addition of various amounts of DMSO showed that minor form gradually transforms into major form.

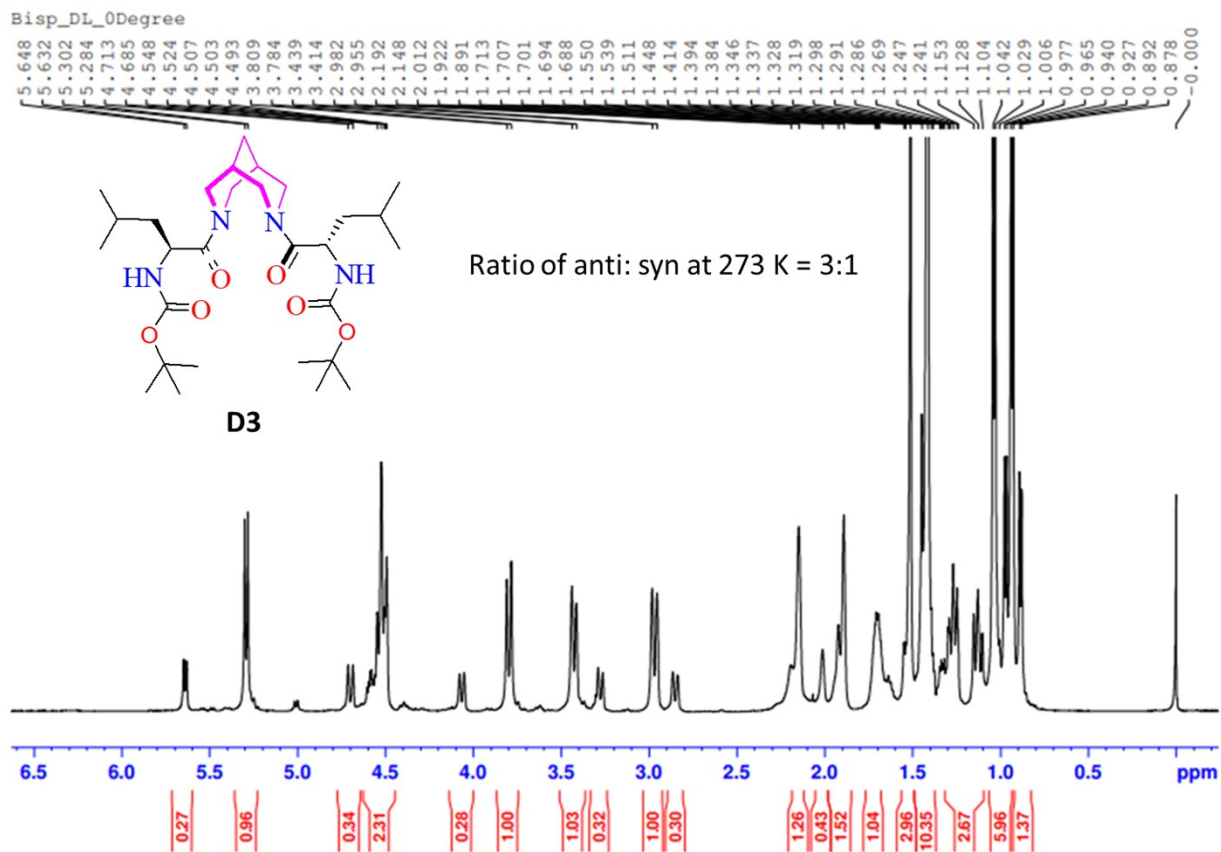


Figure S8: ^1H NMR of **D3** at 273 K shows 1:3 of minor to major form.

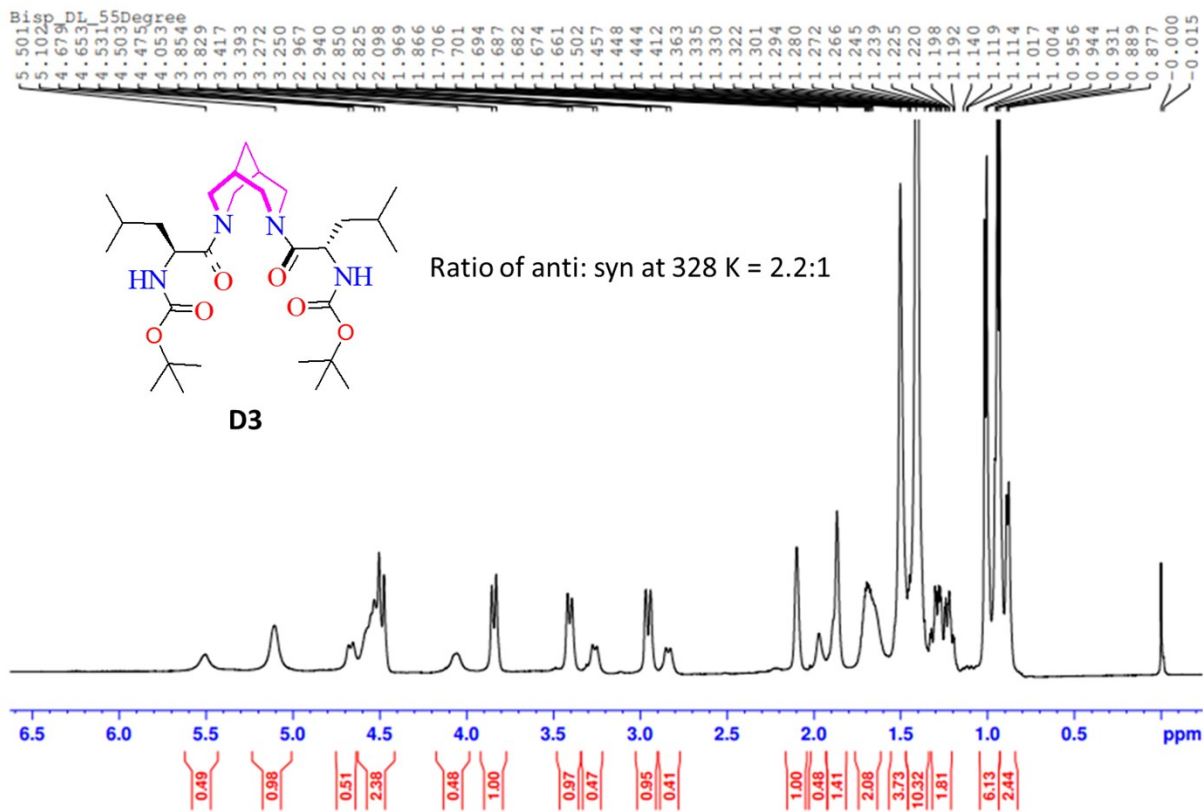


Figure S9: ¹H NMR of **D3** at 328 K shows 1:2.2 of minor to major form.

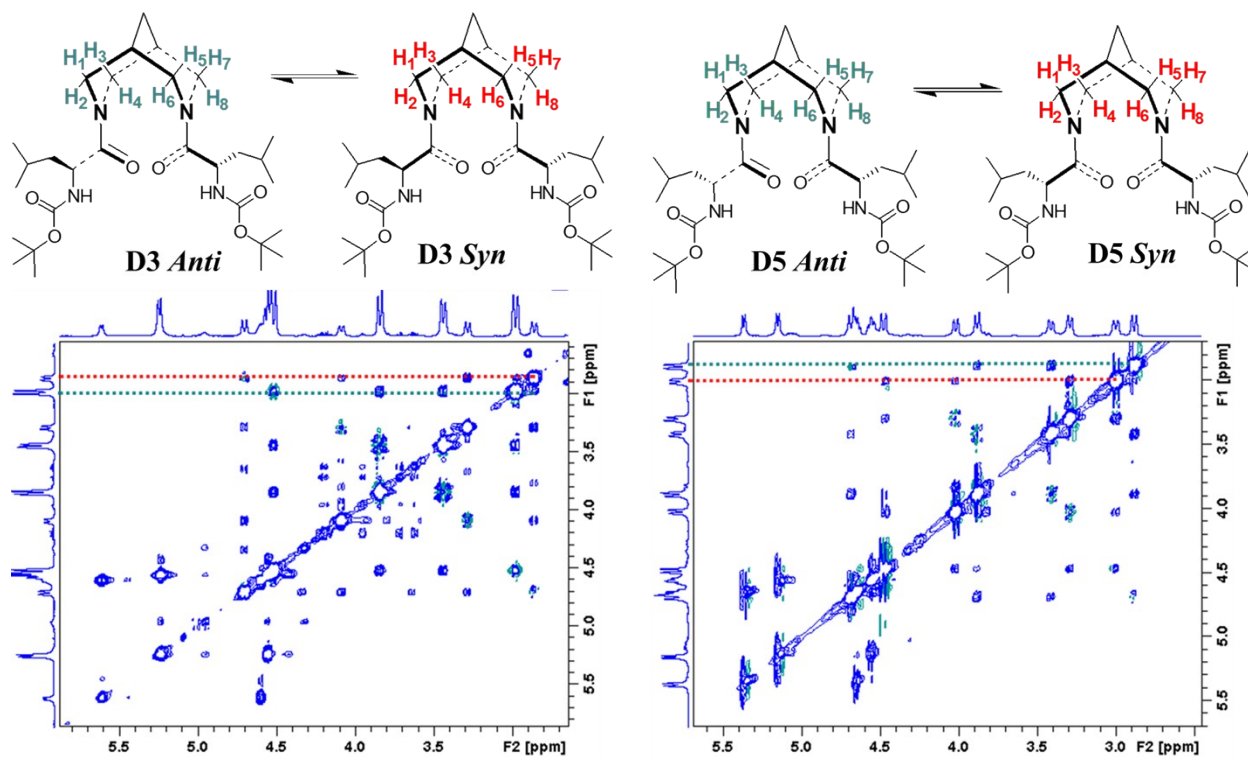


Figure S10: TOCSY spectra of **D3** and **D5** in chloroform showed that both sets of signals are from different conformers.

Selective and non-selective inversion recovery experiments were performed with number of scans = 8, Number of points=4K, Spectral width= 14 ppm on the interested sites with varying mixing delay at each temperature. The signal corresponding to the axial proton of one conformer was inverted using a selective pulse which was calibrated using “paropt” command. The integrated peak area was fitted using MATLAB R2020a for non-selective experiments and using the CIFIT program (specifically designed for exchange data fitting) for selective experiments.

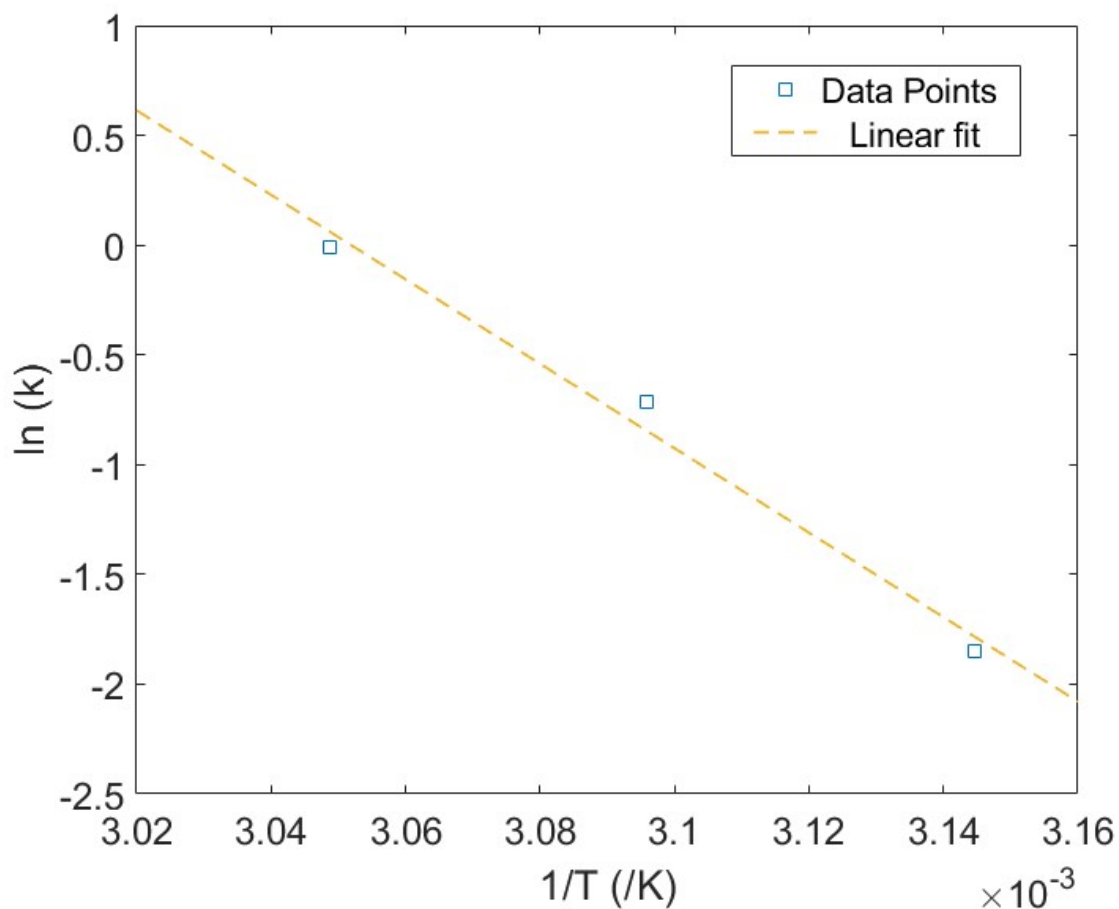


Figure S11a: Plot of $\ln^{\text{rot}}(k)$ against $1/T$ for **D3**. Comparing the value of slope from the fitted equation (dotted line), the activation energy was obtained (mentioned in **Table S3**).

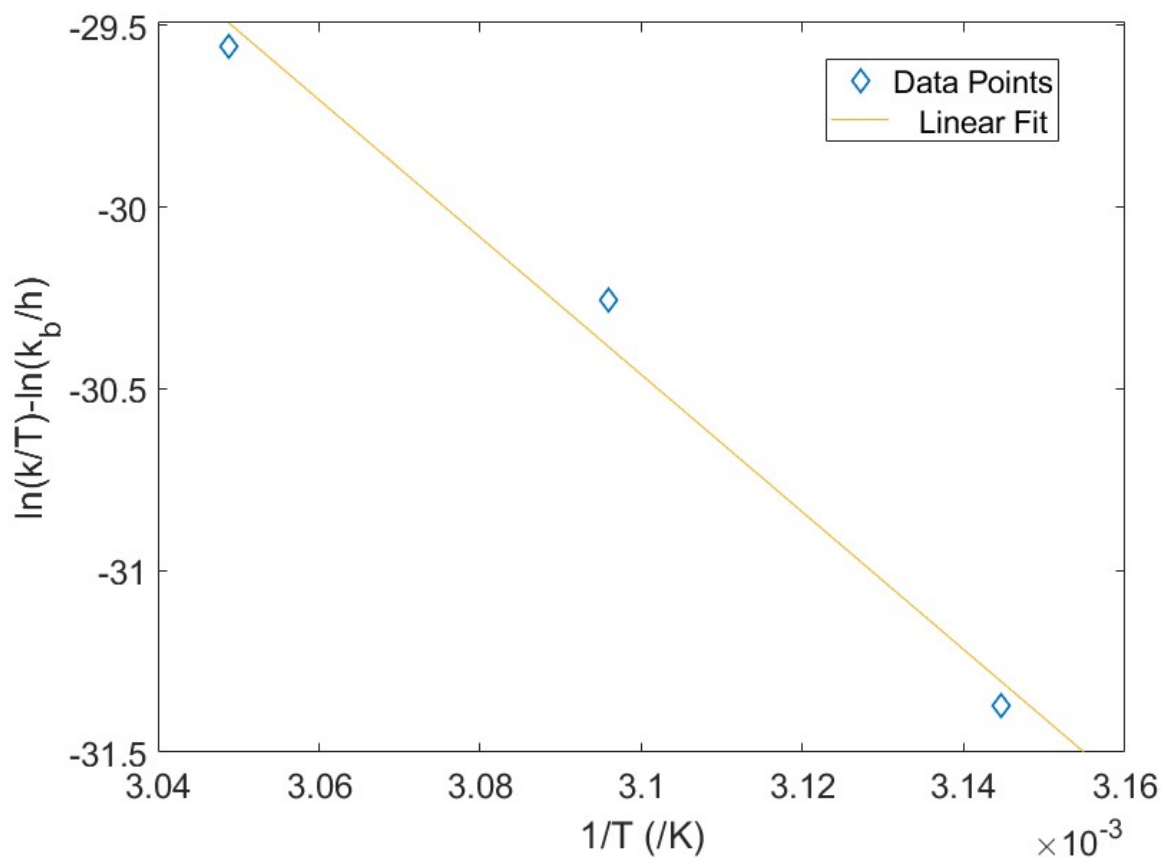


Figure S11b: Plot of $\ln(k/t) - \ln(k_b/h)$ against $1/T$ for **D3**. Comparing the slopes and intercept the values of Enthalpy of activations and Entropy of activation were obtained (mentioned in **Table S3**).

Table S2: Exchange rate data at different temperatures (**D3**).

T(K)	1/T1 of peak at 3.03 ppm (s ⁻¹)	1/T1 of peak at 2.89 ppm (s ⁻¹)	<i>k</i> (s ⁻¹)
308	2.2941	2.2522	-0.1996
313	2.0614	2.0153	-0.0547
318	2.0032	1.9896	0.1674
323	1.8829	1.8761	0.4084
328	1.7724	1.7740	0.8313

Table S3: Energy values for **D3**.

ΔE^\ddagger (kJ/mole)	ΔH^\ddagger (kJ/mole)	ΔS^\ddagger (J/K/mole)
144.41 ± 10.89	141.72 ± 10.89	184.26 ± 33.67

The fitted data is shown in **Figure S11c**. The solid line shows the inverted peak of one conformer and dotted line is the exchanging counter part of the former peak (Normalized intensity). The exchange effect can be seen on the exchange peak in initial part of the time.

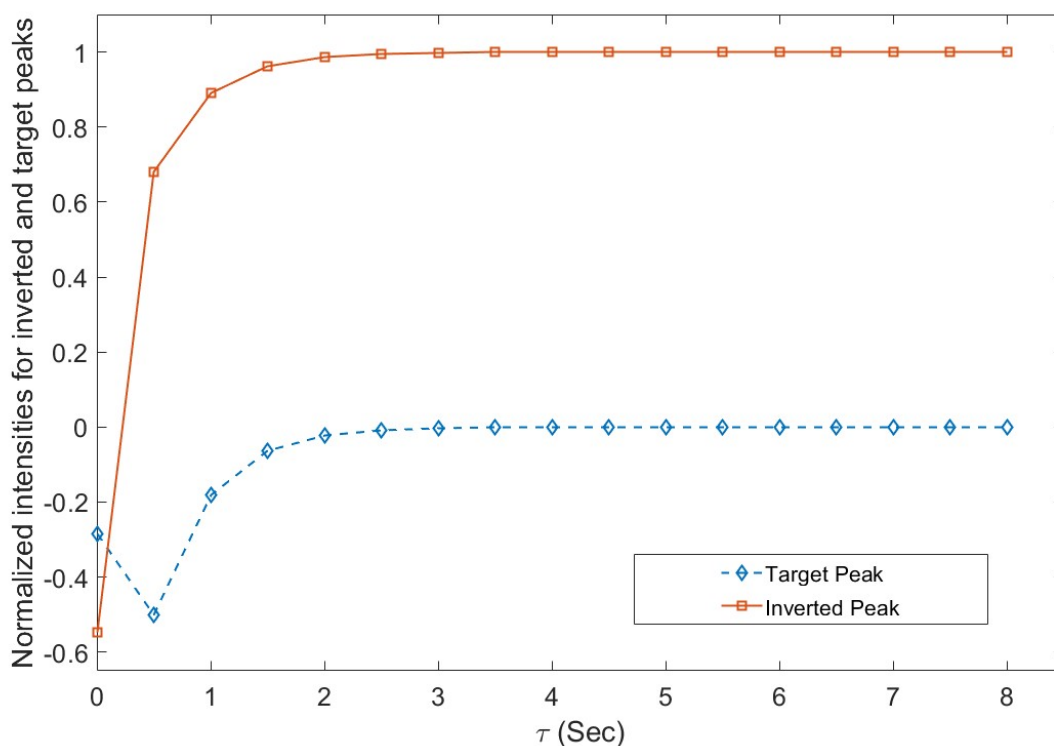


Figure S11c: Plot of normalized intensities of the inverted peak (solid line) and target peak (dotted line) against the mixing delay varied at 35 °C.

These profiles are fitted for these peaks at several temperatures to get the exchange rate (k). The summarized data is given below in **Table S4**. The temperature range is taken from 278K-303K.

Table S4: Exchange rate data at different temperatures (D5).

T(K)	1/T1 of peak at 3.03 ppm (s ⁻¹)	1/T1 of peak at 2.89 ppm (s ⁻¹)	<i>k</i> (s ⁻¹)
303	2.4160	2.3557	0.3065
308	2.2941	2.2522	0.8030
313	2.0614	2.0153	1.5992
318	2.0032	1.9896	3.3570
323	1.8829	1.8761	6.2875
328	1.7724	1.7740	10.7850

Arrhenius plot of $\ln(k)$ vs. $1/T$ gives the activation energy, ΔE^\ddagger , because:

$$k = A \exp\left(-\frac{\Delta E^\ddagger}{RT}\right)$$

where A is the pre-exponential factor, R is the gas constant. (Figure S12d)

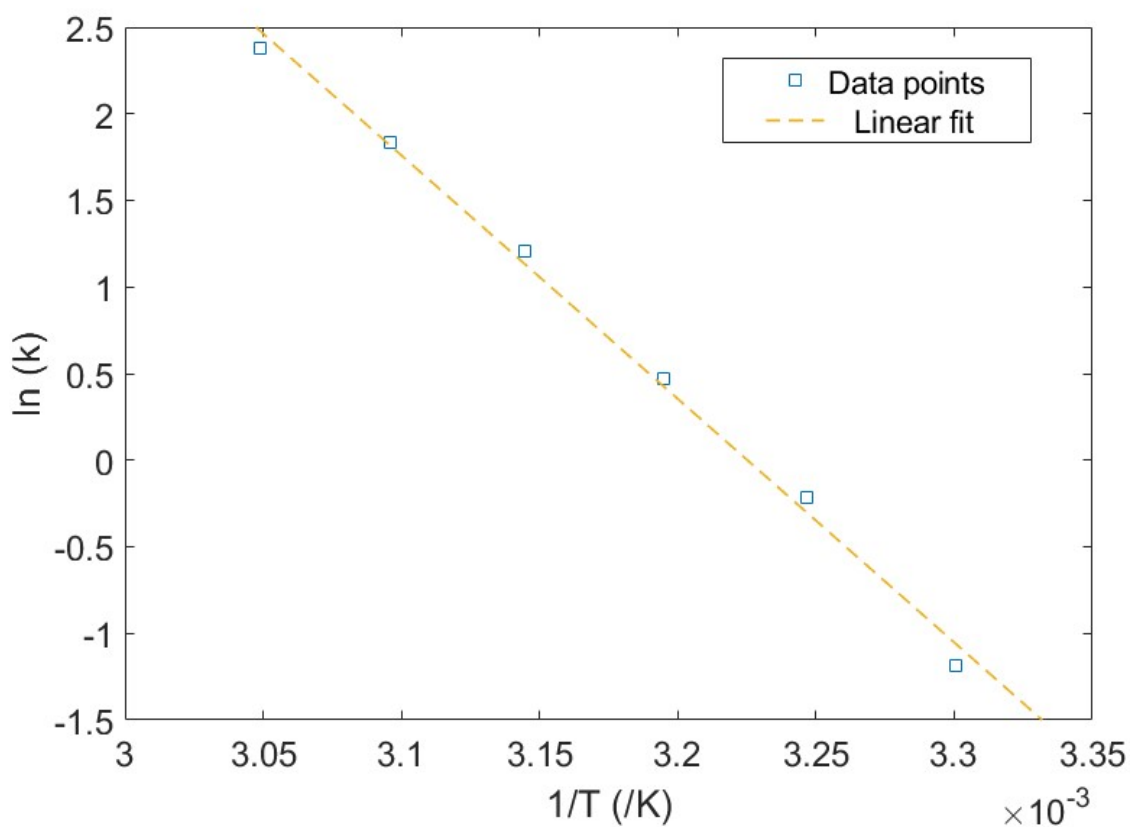


Figure S11d: Plot of $\ln(k)$ against $1/T$ D5. Comparing the value of slope from the fitted equation (dotted line), the activation energy was obtained (mentioned in Table S5).

Also, Eyring plot gives the enthalpy of activation and entropy:

$$k = \frac{k_B T}{h} \exp\left(-\frac{\Delta G^\ddagger}{RT}\right)$$

$$k = \frac{k_B T}{h} \exp\left(\frac{\Delta S^\ddagger}{R} - \frac{\Delta H^\ddagger}{RT}\right)$$

where, k_B is the Boltzmann's constant, h is Planck's constant, ΔG^\ddagger is the free energy of activation, ΔS^\ddagger is the entropy of activation and ΔH^\ddagger is the enthalpy of activation. The fit is shown in **Figure S12e**.

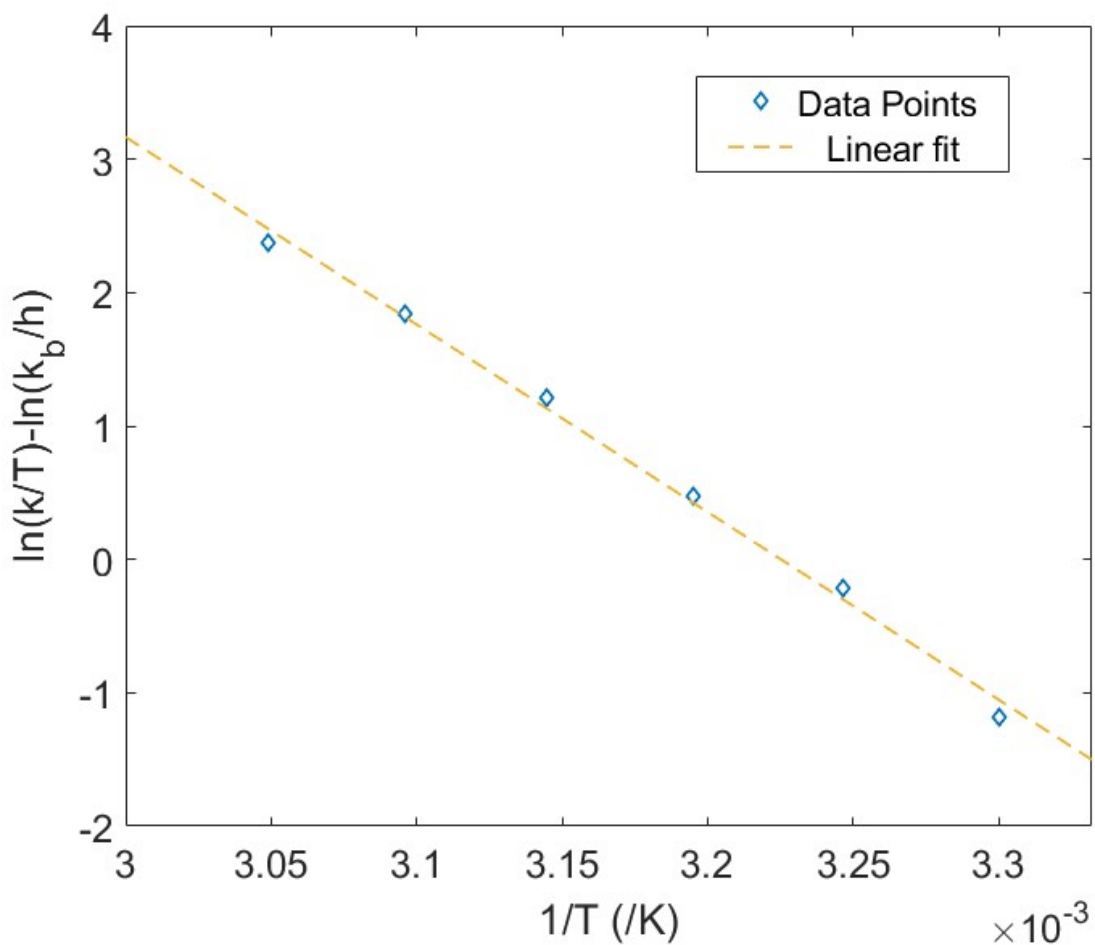


Figure S11e: Plot of $\ln(k/t) - \ln(k_b/h)$ against $1/T$ **D5**. Comparing the slopes and intercept the values of Enthalpy of activations and Entropy of activation were obtained (mentioned in **Table S5**).

Values obtained are as follows:

Table S5: Energy values for **D5**.

ΔE^\ddagger (kJ/mole)	ΔH^\ddagger (kJ/mole)	ΔS^\ddagger (J/K/mole)
116.92 ± 4.04	114.3 ± 4.06	123.41 ± 12.89

2. Computational modelling

2.1 ω torsional angle scan using DFT

The potential energy of the molecules **D1** and **D2** was calculated for every 10° change in the dihedral angle of the amide bond between the bispidine nitrogen and the carbonyl atom of the connecting group on both arms of the linker (ω_1 and ω_2). ORCA² quantum chemistry package was used for geometry optimization at the DFT level for every dihedral configuration using the default convergence criteria (here a convergence of < 0.1 kT between successive geometry optimization steps for all structures was achieved). CAM-B3LYP/6-31G* functional basis set was applied for the DFT calculations and the default Quasi-Newton BFGS optimization algorithm was used for geometry optimization. The following torsional angles were used as reaction coordinates to study the isomerisation (see **Figure S2.1** for nomenclature):

	ω_1	ω_2
D1	O4-C11-N2-C8	O5-C12-N3-C9
D2	O4-C12-N2-C19	O5-C12-N3-C20

2.2 Weighted Ensemble simulations

2.2.1 Setup

All-atomistic molecular dynamics simulations of **D3** and **D5** were performed using the Weighted Ensemble (WE) sampling strategy. The structure of **D3** was taken from the XRD resolved data. Leucine residue on one arm (atoms around C11) was inverted using PyMol³ to convert the L enantiomer to D form. Molecule topologies were generated from CGENFF⁴ implementation of the CHARMM36FF for small molecules. Simulations were performed using the GROMACS 2021 software⁵. The molecules were placed in a dodecahedral box such that the starting structures were at least 1.5 nm away from the edges of box. The box was solvated with chloroform (CHCl₃). The topology and GRO files of chloroform were generated using SWISS-PARAM⁶ (CHARMM22FF). The number of solvent molecules was decided based on the empty volume in the box while assuming a density of 1478 g/L of chloroform. The solvated system was energy-minimized (EM) using the steepest-descent algorithm until the maximum forces are < 1000 kJ/mol. To generate the correct velocities, we performed simulated annealing (SA) for 500 ns by raising the temperature of the system from 10K to 328 K. This was followed by equilibration in the NVT ensemble at 328K for 500 ns. Berendsen thermostat was used in SA and NVT steps with separate coupling constants for solute ($\tau_T = 0.5$ ps) and solvent ($\tau_T = 0.1$ ps). Position restraints on the backbone and linker heavy atoms (force constant $k=1000$ kJ/mol nm²) were applied during the EM, SA and NVT steps. The final equilibration step in the NPT ensemble was performed for 1 ns without position restraints using the Berendsen thermostat (solute $\tau_T = 1$ ps, solvent $\tau_T = 0.5$ ps) and barostat ($\tau_P = 4$ ps). The equilibrated box was subjected to a 100 ns of Well-Tempered Metadynamics (metaD)

to generate an ensemble of structures for the WE initialization. The dihedral angles of linker-leu peptide bonds from both arms were used as two collective variables for metaD simulations, viz. $\omega_1 = \text{O30-C2-N31-C19}$ and $\omega_2 = \text{O29-C3-N23-C1}$.

2.2.2 WE Set-1

The first set of WE simulations were performed by binning in two dimensions along the ω torsional angles of both arms of the linker as progress coordinates ($\omega_1 = \text{O30-C2-N31-C19}$ and $\omega_2 = \text{O29-C3-N23-C1}$). **D3** and **D5** share identical atom numbers (labelled in **Figure S12 c, d**). Structures for initialization of WE were taken at every 10° intervals of the ω torsion from metaD simulations such that entire ω torsional space is spanned (-180° - 180°) resulting in 1201 walkers for **D3** and 911 walkers for **D5** out of a possible 1296 (36×36). A resampling time of 25 ps for each iteration was used. The number of walkers per bin were set to seven. A recursive binning scheme was used such that the region involving transitions ($-130^\circ < \omega < 130^\circ$) was adaptively binned with 20 bins while using fixed binning for the remainder.⁷ All simulations were performed at 328 K and 1 bar (NPT ensemble) for a total number of 100 WE iterations. The simulation was performed in the isothermal-isobaric ensemble (NPT) using the Parrinello-Rahman barostat and v-rescale thermostat ($\tau_p = 10$ ps and solute $\tau_T = 1$ ps, solvent $\tau_T = 0.5$). Further details on the setup are provided in the attached configuration and parameter files.

2.2.3 WE Set-2

The second set of simulations were initialized by taking intermediate walkers (not belonging to *syn* or *anti* states) from the last iteration (100th) of set-1. Two sets of simulations for **D3** with initial walkers one in the intermediate region of *syn* \rightarrow *anti*' and the other involving *syn* \rightarrow *anti* were performed. Only the *syn* \rightarrow *anti* transition was studied for **D5**. For obtaining *syn* \rightarrow *anti* events from WE, a single bin was used in the region outside the interest of the transition for the ($-\infty < \omega_1 < -140^\circ$) and 25 bins were applied when ω_1 lies in between -140° and 140° such that binning adaptively favors higher values of ω_1 . A smaller number (10 adaptive bins) were used along ω_2 (in 50° - 140°). 300 iterations were performed using a resampling time of 10 ps, leading to a 3 ns of molecular time. Refer to the attached files for further details.

2.2.4 WE calculations and analysis

1. The progress coordinate was calculated by adding 90° to the measured ω dihedral angle. This shifting was done to remove periodicity in the state definitions.
2. State definitions: Anti: $50^\circ < \omega_1 < 130^\circ$, $50^\circ < \omega_2 < 130^\circ$, Anti': $-130^\circ < \omega_1 < -50^\circ$, $-130^\circ < \omega_2 < -50^\circ$, Syn: $-130^\circ < \omega_1 < -50^\circ$, $50^\circ < \omega_2 < 130^\circ$, Syn': $50^\circ < \omega_1 < 130^\circ$, $-130^\circ < \omega_2 < -50^\circ$.

3. The free energy of a bin ' i ' in a progress-coordinate space given the weight of the walkers in the bin (w_i) is calculated as $-\ln(w_i)$ (units in kJ/mol). The weights of walkers sum in a WE simulation sum to 1.

4. To calculate the rate of the $syn \rightarrow anti$ transition, the weight of those walkers entering the *anti*-state given their most-recent history (parent trajectories) in the *syn* state for every iteration is counted. This measure called $syn \rightarrow anti$ conditional flux, is averaged over the last 200 iterations and the rate is thus calculated as:

$$k_{Syn \rightarrow Anti} = \frac{\sum_i^N \sum_j^n w_{ij}^S}{N \cdot \tau} \cdot \frac{1}{\frac{\sum_i^N \sum_j^n w_{ij}^{Syn}}{N}} \quad (S1)$$

where,

N: Number of iterations.

n: number of walkers in iteration i .

w^S : Weight of walkers with recent most recent history in *syn* that enter *anti* state in iteration i .

τ : Resampling time.

w^{Syn} : Weight of walkers in *syn* state in iteration i .

2.3 Well-Tempered Metadynamics

A Well-Tempered Metadynamics (metaD) simulation⁸ was performed for **D5** using the ω_1 (O30-C2-N31-C19, L-Leu) and ψ_1 (24N-12C-2C-31N, L-Leu) torsional angles as collective variables. A trajectory was generated until the free energy surface was converged (1 μ s). Gaussians ($\sigma=0.05$) with a bias factor of 10 with an initial height of 1kJ/mol were deposited every 500 time steps (1 ps). Similar equilibration steps as described in Section S2.2.1 were adopted. The simulation was performed in the isothermal-isobaric ensemble (NPT) using the Parrinello-Rahman barostat and v-rescale thermostat ($\tau_p = 10$ ps and solute $\tau_T = 1$ ps, solvent $\tau_T = 0.5$).

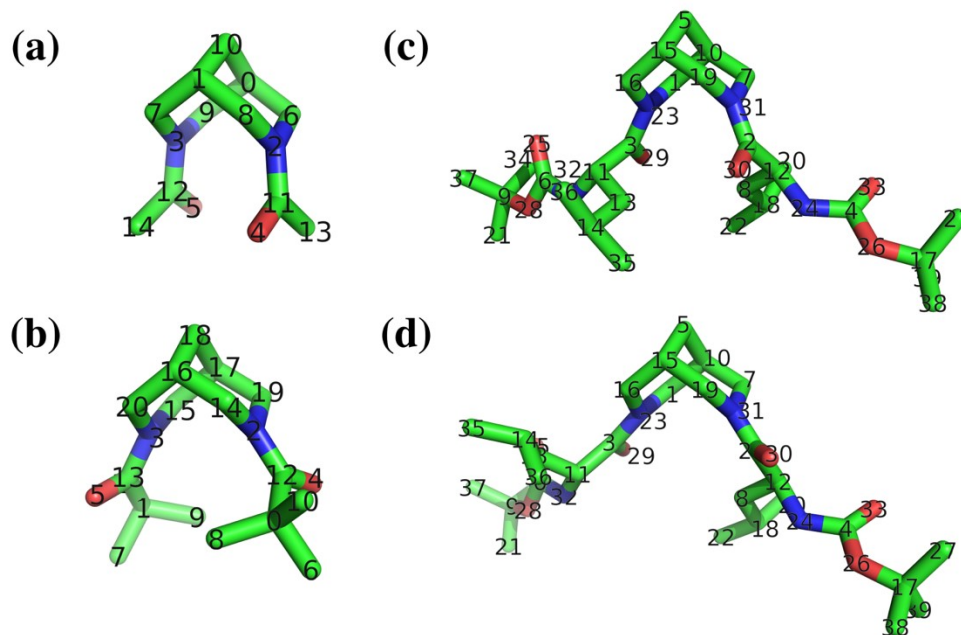


Figure S12: Structures of **D1**, **D2**, **D3** and **D5** respectively. **D2** and **D3** are X-ray resolved crystal structures while **D1** and **D5** were modified in-silico (**Section 2.2**). The atom numbering follows the topologies generated from CGENFF. The same index scheme was used for defining the reaction coordinates in DFT, WE and metaD simulations.

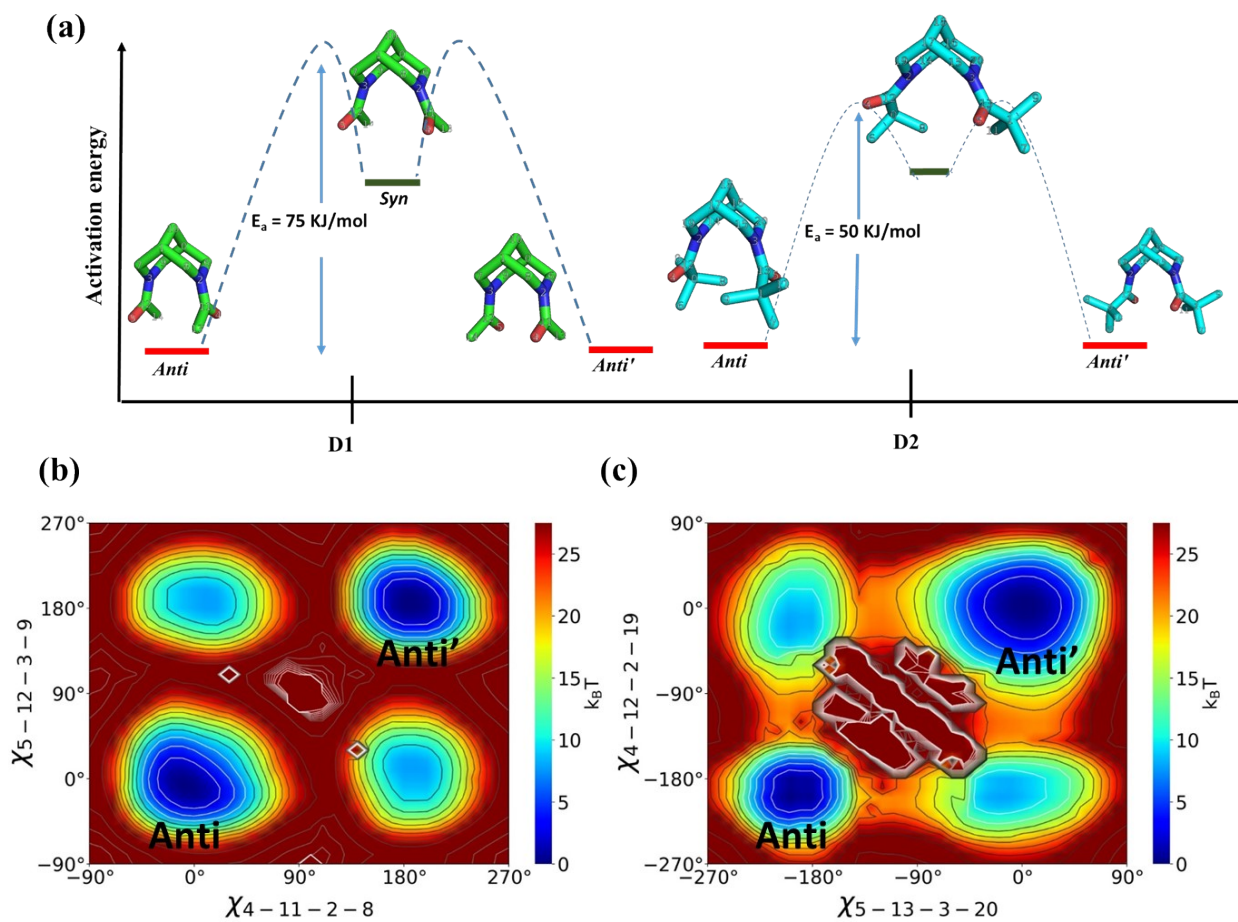


Figure S13: A pictorial representation of the energy profile of **D1** and **D2** based on DFT calculation. (a, b) Potential energy surface of **D1** and **D2**. The ω dihedral angle of the arms are chosen as the reaction coordinates for studying the isomerization. The contours are plotted for every 12.5 kJ/mol increment in the potential energy. Details of DFT scans and geometry optimization are elaborated in **Section S2.1**.

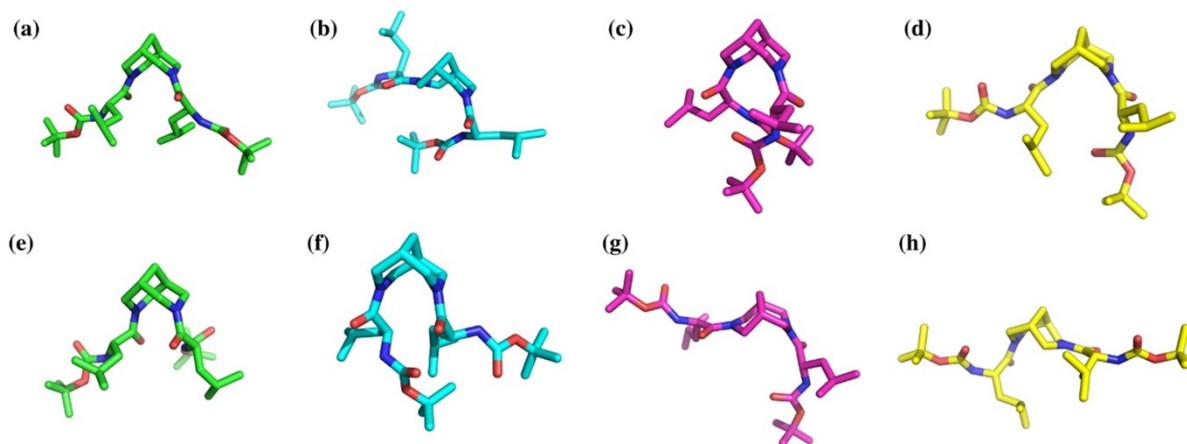


Figure S14: Structures of **D3** and **D5** sampled from WE simulations. Figures (a,e) (in green) represent the *anti*-conformation of **D3** and **D5** respectively while the structures in (c,g) are the corresponding *anti'* states. The structures in cyan (b,f) denote the *syn* state and the yellow colored poses (d,h) belong to the *syn'* state of corresponding **D3** and **D5** molecules. The state definitions are mentioned in **Section 2.2.4.2**.

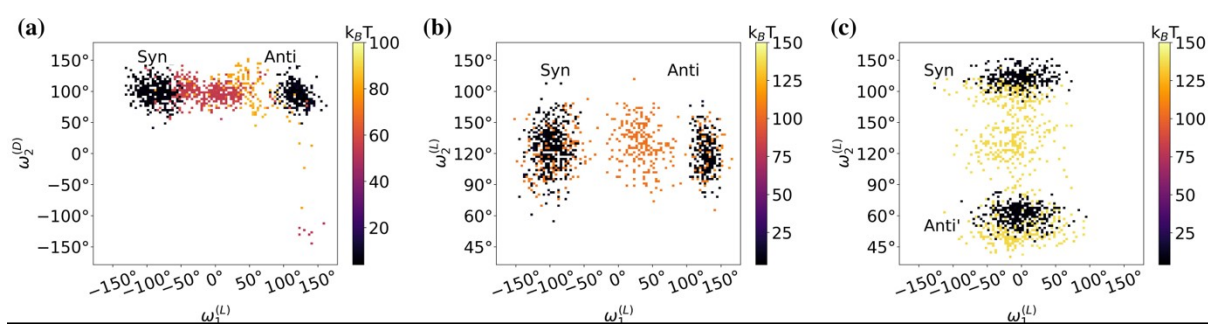


Figure S15: Free energy surface (FES) from WE set-2 simulations. (a) is the FES of **D5** obtained on studying the *syn*→*anti* transition by finer binning along ω_1 and restricting sampling along ω_2 by coarser bins. The same is shown for **D3** in figure (b). (c) depicts the FES of **D3** for the *syn*→*anti* transition, with finer bins along ω_2 and coarser along ω_1 . The colour represents the free energy (in kJ/mol) of the walkers after 300 iterations of WE (3ns of molecular time).

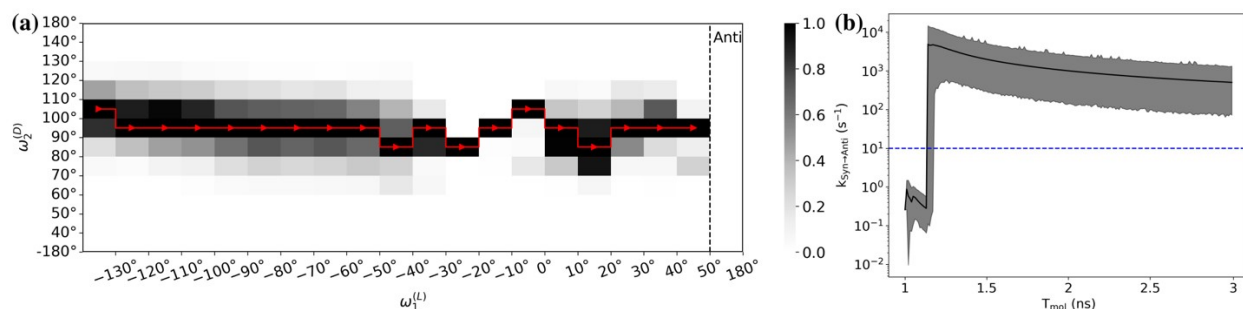


Figure S16: (a) The figure illustrates the relative weight of the walkers along ω_2 for a given ω_1 (**D5**). An interval of 10° was used as spacing between the bins for estimation of the relative weights. The curve highlighted in red represents the minimum free energy path (highest relative weight) for the *syn*→*anti* isomerization. (b) The rate of the *syn*→*anti* isomerization directly calculated from successful transition events from WE set 2 simulation of **D5**. The blue dashed line represents the estimate rate from NMR relaxation experiments (**Table S4**). Rate calculation from WE is given by **Equation S1**. Transition events only after 1ns of molecular time were considered for calculation of the minimum energy path and rates.

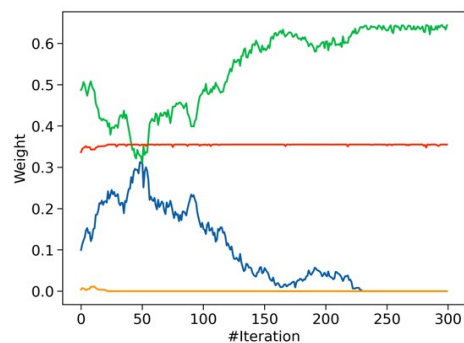


Figure S17: The figure plots the time evolution of the weights of the sub-ensembles of the states from WE set 2 simulations of **D5**. The green curve denotes the *syn* state in β -region and the blue curve denotes the *syn* state in α -region. The red curve is the population evolution of the *anti- β* state and the orange curve represents the *anti- α* state. The average populations over the last 200 iterations are 0.623, 0.016, 0.355, 6.876e-13 respectively and 0.638, 0.355, 1.2e-17 and 7.5e-20 respectively when averaged over the last 50 iterations.

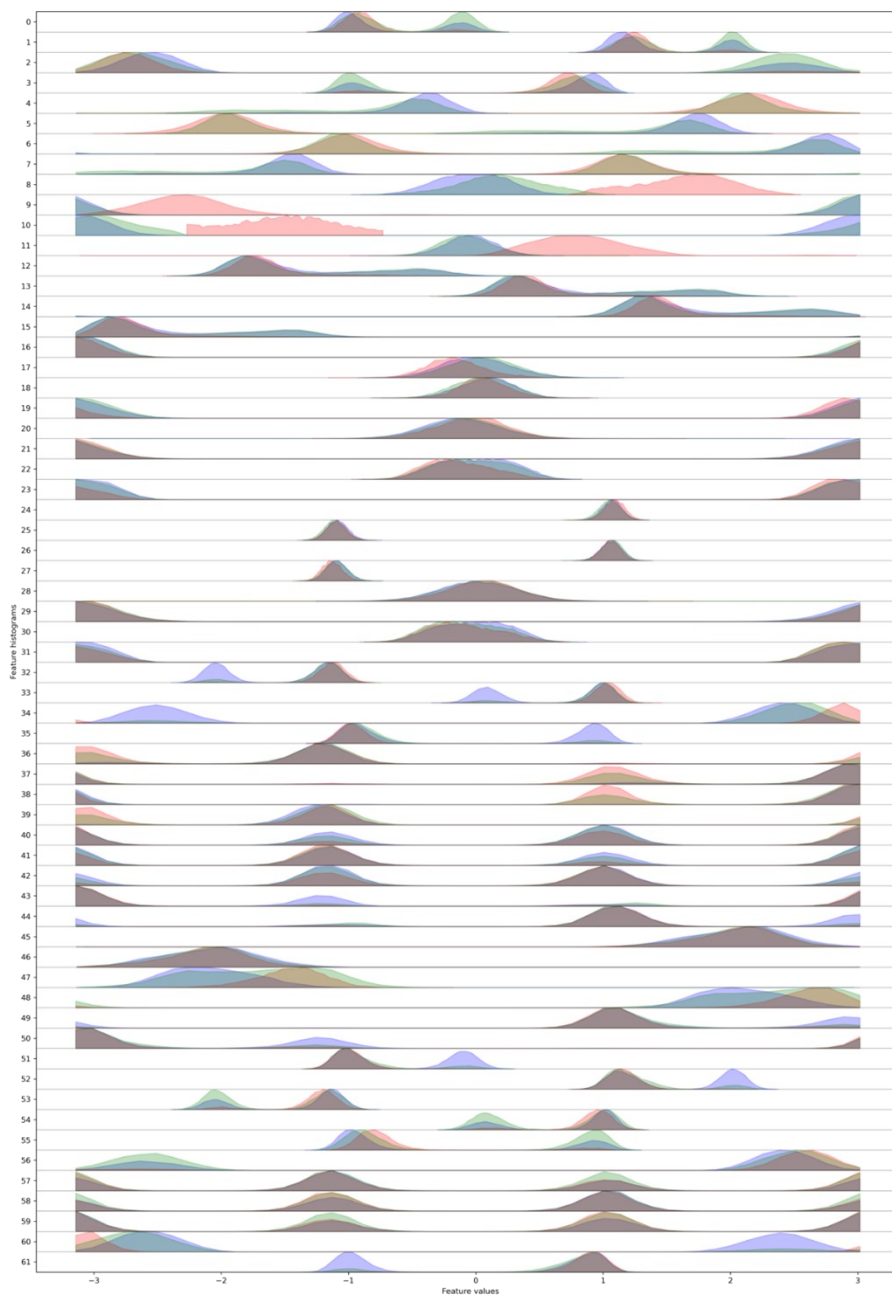


Figure S18: Histograms of all possible heavy-atom torsional angles of **D5** from WE simulations. The colors denote three sub-ensembles viz, blue: walkers in the *syn* state initialized from the *syn* state (i.e. *syn* states with a history in the *syn* state at iteration #0), red: walkers in the intermediate region (between *syn* and *anti* ($-50^\circ < \omega_1 < 50^\circ$)) initialized from the intermediate region and green: *syn* states initialized from the intermediate region. The atom quadruples denoting the 62 dihedrals are provided as an attachment. Dihedral #6 denotes the $\psi_1^{(L)}$ of the L-leu arm of **D5**. The green dihedral shows two peaks, one belonging to the α -helical ($-1.75 < \psi < 0.17$) region and the other belonging to β region ($1.04 < \psi < 3.49$). The sub-ensemble belonging to the α region was observed in successful isomerization events to the *anti*-state.

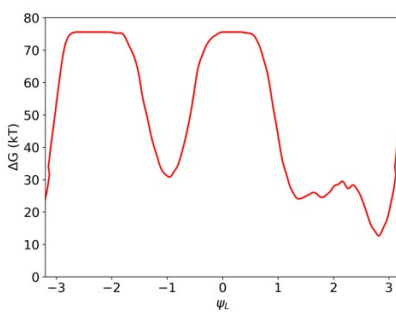


Figure S19: The projection of the free energy surface from metaD simulation of **D5** (Section 2.3) for the *syn* state. It is observed that a larger barrier exists for the β region ($1.04 < \psi < 3.49$) to the α region ($-1.75 < \psi < 0.17$) conformation (~ 164 kJ/mol) than the reverse transition ($\alpha \rightarrow \beta$, ~ 122 kJ/mol).

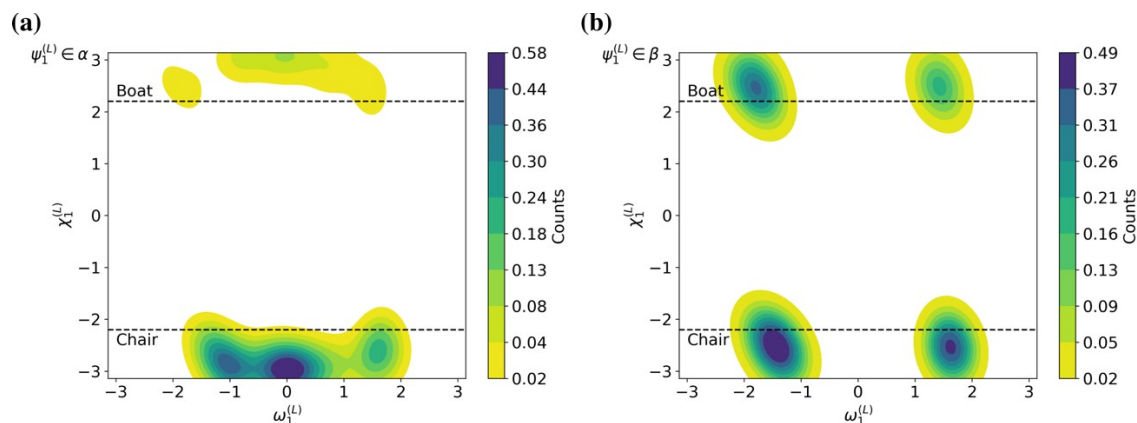
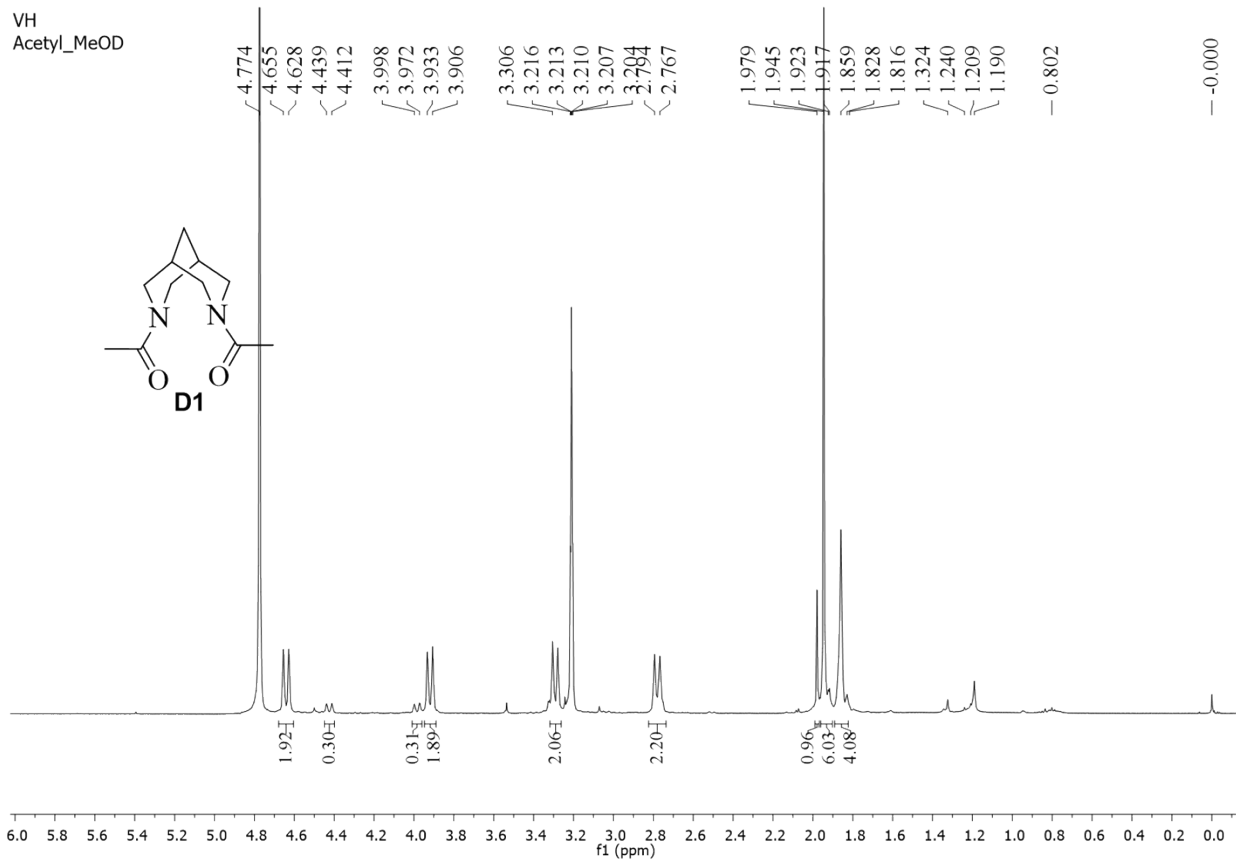


Figure S20: A 2D distribution of count of walkers in the WE ensemble simulation of **D5** projected along the ω_1 and the χ_1 torsion. The ω_1 torsion separates the syn and anti states and the χ_1 torsion (C15-C19-N31-C2 as per Figure S12d) separates the chair-chair and the chair-boat conformations. (a) and (b) correspond to the data for the α and β sub-ensembles (ψ_1 L-leu), respectively. The continuous distribution was obtained from the discrete counts in 2D bins, with total count equal to 118905 and 126102 in the α and β sub-ensembles, respectively.

Data and code availability

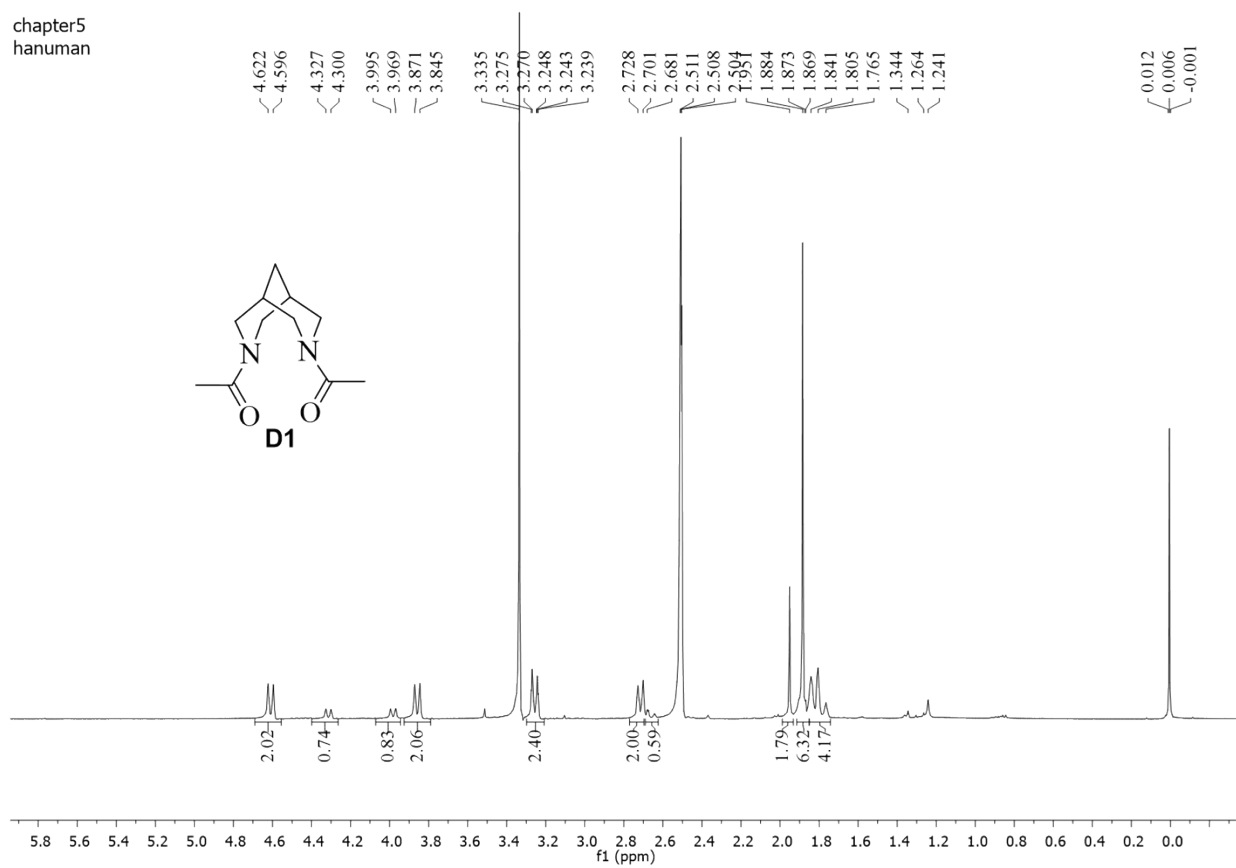
Files containing the structures, topologies, simulation parameters and analysis are provided in <https://github.com/akshay-chenna/Bispidine2>.

VH
Acetyl_MeOD

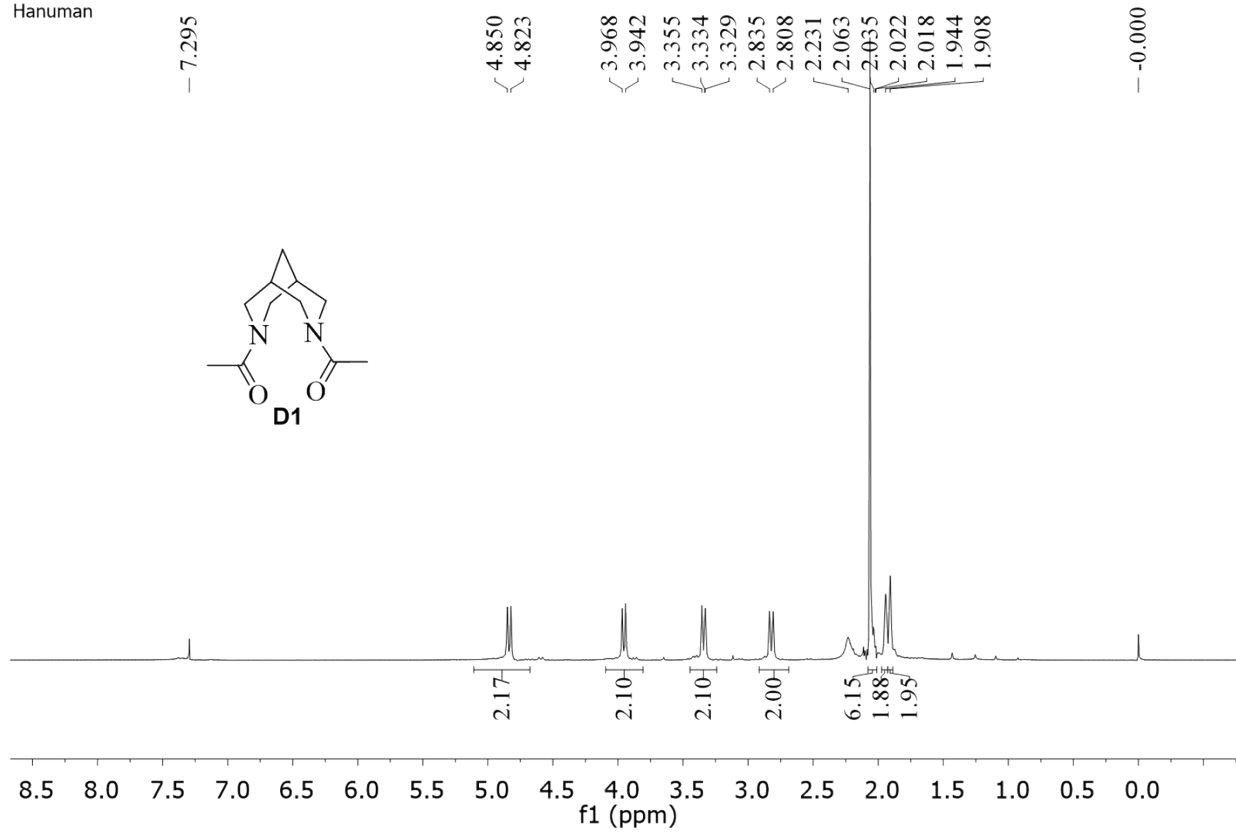


¹H NMR (500 MHz, CD₃OD) of **D1**

chapter5
hanuman



Hanuman
Hanuman



^1H NMR (500 MHz, CDCl_3) of **D1**

Hanuman
Hanuman

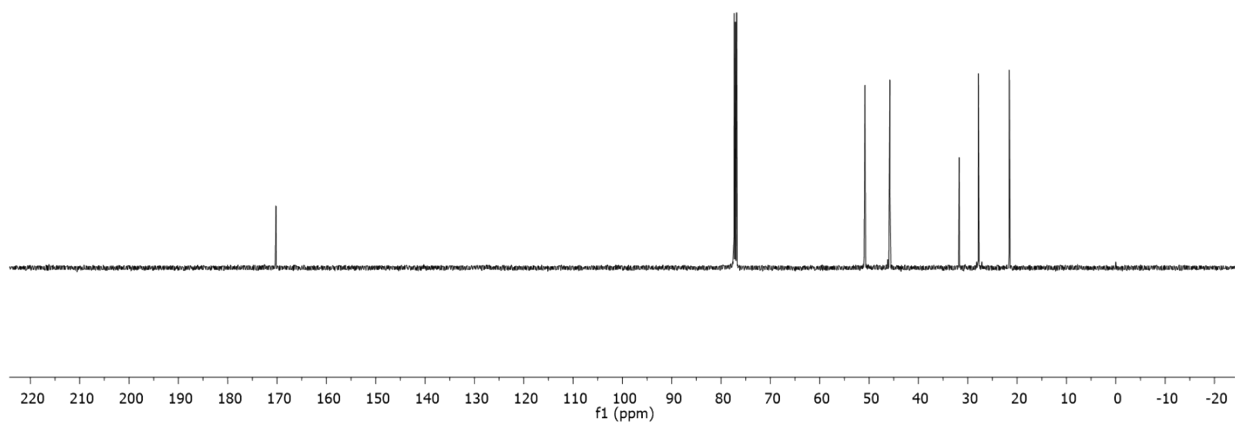
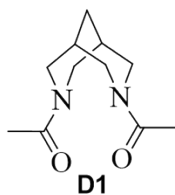
— 170.213

{ 77.348
77.095
76.840

— 50.840
— 45.794

— 31.736
— 27.837
— 21.592

— -0.000



¹³C NMR (125 MHz, CDCl₃) of **D1**

Mass Spectrum SmartFormula Report

Analysis Info

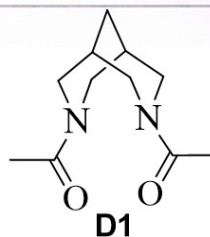
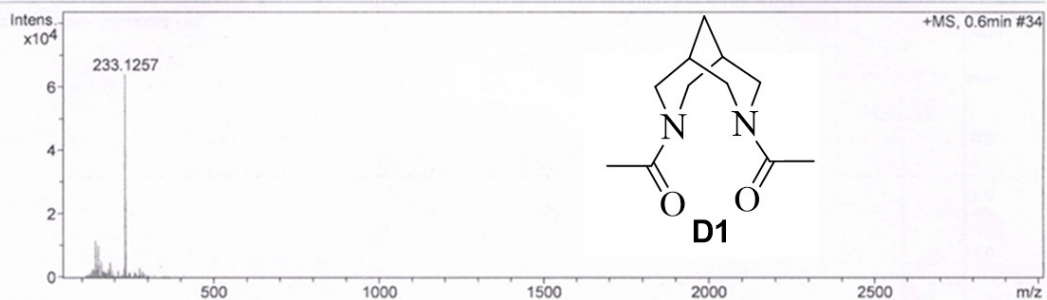
Analysis Name Y:\Data\DEC 2021\wh r 7000001.d
Method Tune_Low_New.m
Sample Name tm 1 100
Comment

Acquisition Date 12/23/21 3:49:44 PM

Operator BDAL@DE
Instrument micrOTOF-Q 228888.10262

Acquisition Parameter

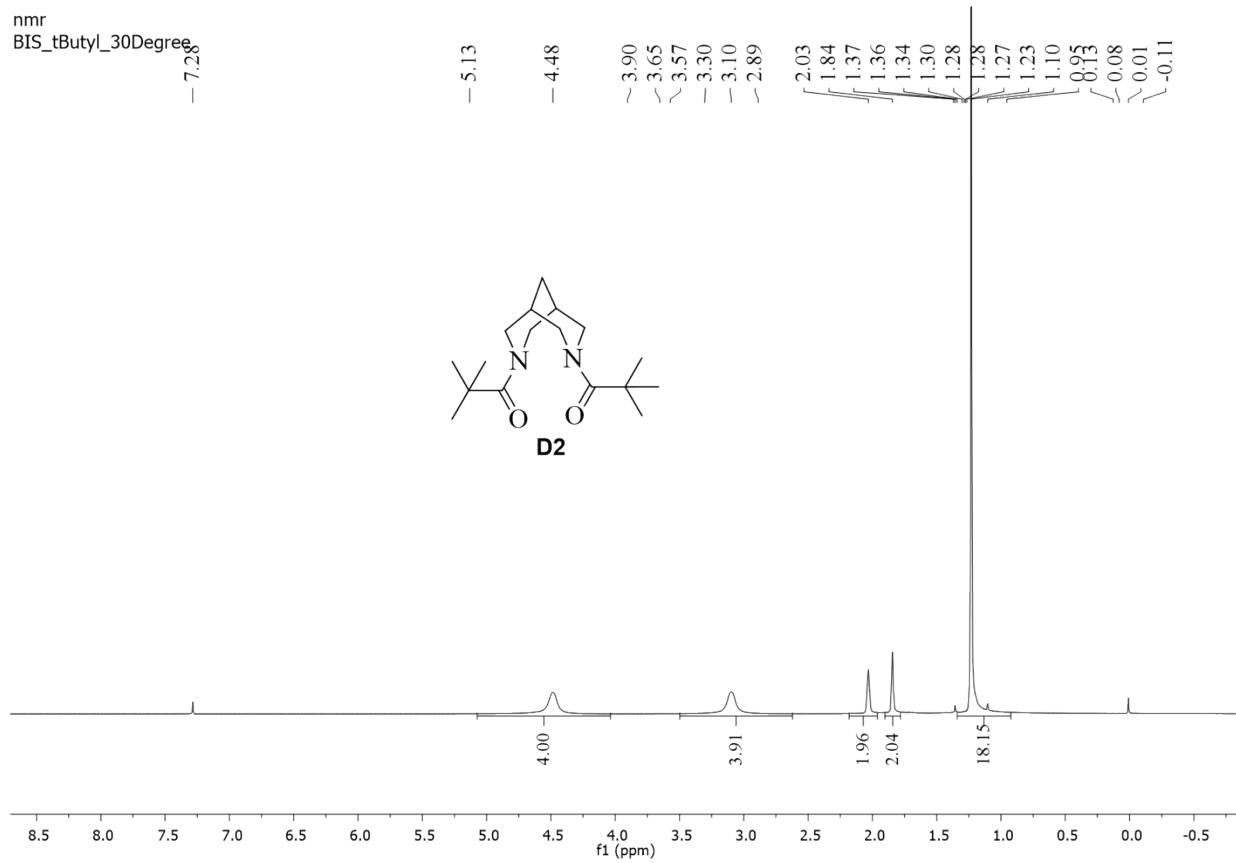
Source Type	ESI	Ion Polarity	Positive	Set Nebulizer	0.4 Bar
Focus	Active	Set Capillary	4500 V	Set Dry Heater	180 °C
Scan Begin	50 m/z	Set End Plate Offset	-500 V	Set Dry Gas	4.0 l/min
Scan End	3000 m/z	Set Collision Cell RF	200.0 Vpp	Set Divert Valve	Source



Meas. m/z	#	Ion Formula	m/z	err [ppm]	mSigma	# mSigma	Score	rdb	e ⁻ Conf	N-Rule
233.1257	1	C ₁₁ H ₁₈ N ₂ NaO ₂	233.1260	1.5	2.3	1	100.00	3.5	even	ok

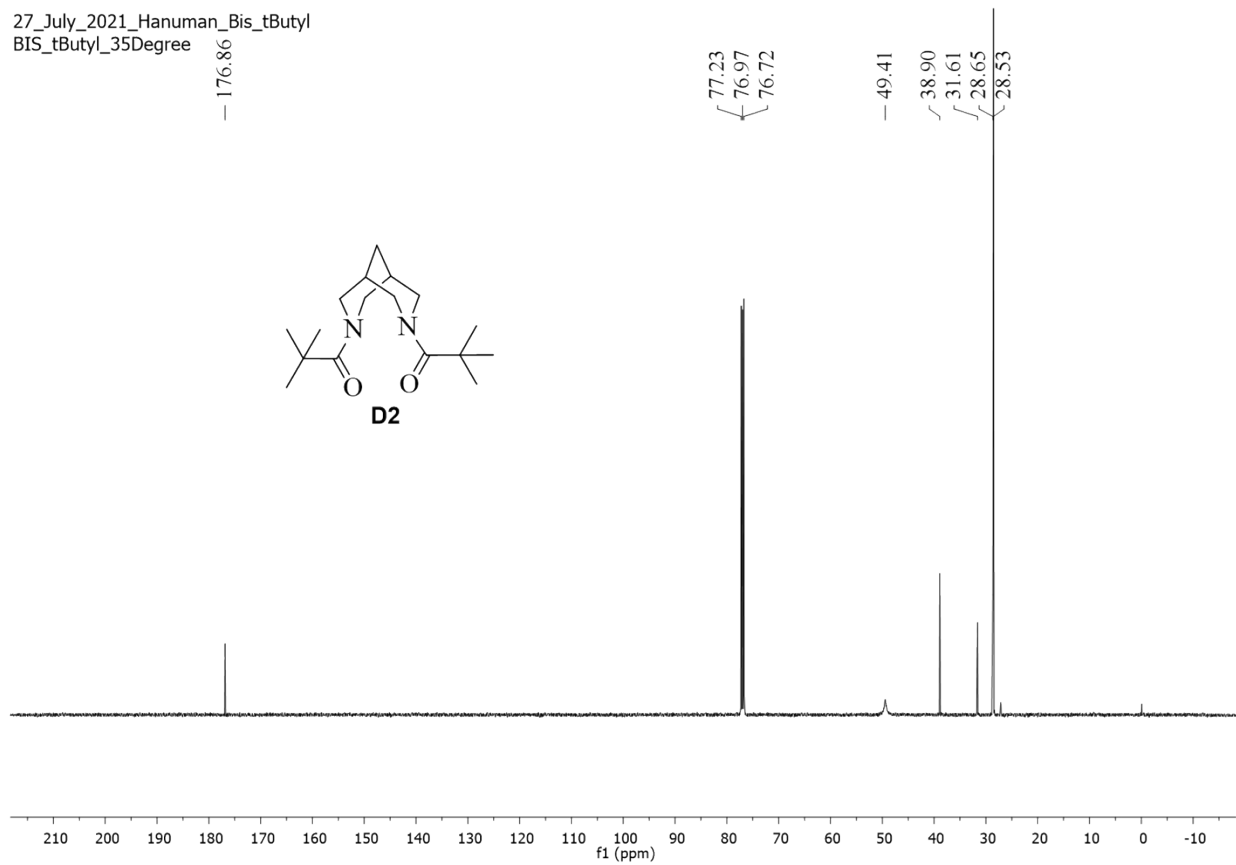
HRMS of **D1**

nmr
BIS_tButyl_30Degree



¹H NMR (500 MHz, CDCl₃) of **D2**

27_July_2021_Hanuman_Bis_tButyl
BIS_tButyl_35Degree



^{13}C NMR (125 MHz, CDCl_3) of **D2**

Mass Spectrum SmartFormula Report

Analysis Info

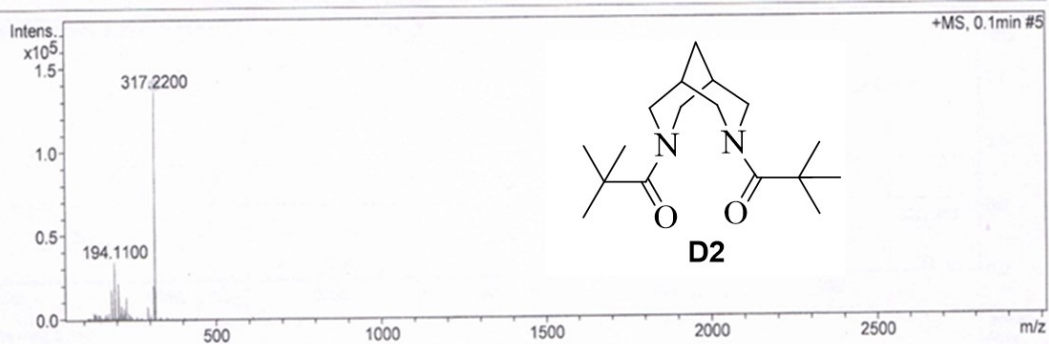
Analysis Name Y:\Data\DEC 2021\wh r 6 r000001.d
Method Tune_Low_New.m
Sample Name tm 1 100
Comment

Acquisition Date 12/23/21 3:52:25 PM

Operator BDAL@DE
Instrument micrOTOF-Q 228888.10262

Acquisition Parameter

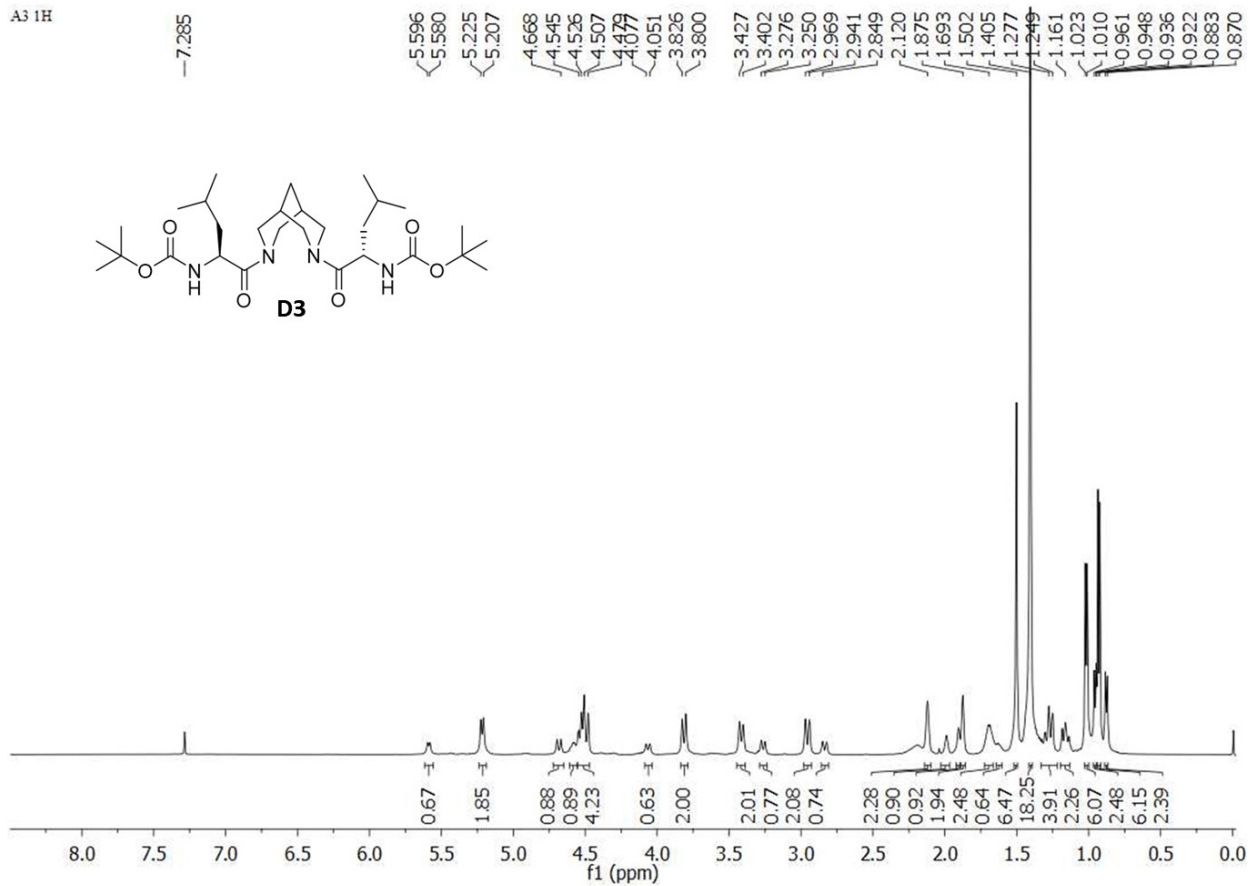
Source Type	ESI	Ion Polarity	Positive	Set Nebulizer	0.4 Bar
Focus	Active	Set Capillary	4500 V	Set Dry Heater	180 °C
Scan Begin	50 m/z	Set End Plate Offset	-500 V	Set Dry Gas	4.0 l/min
Scan End	3000 m/z	Set Collision Cell RF	200.0 Vpp	Set Divert Valve	Source



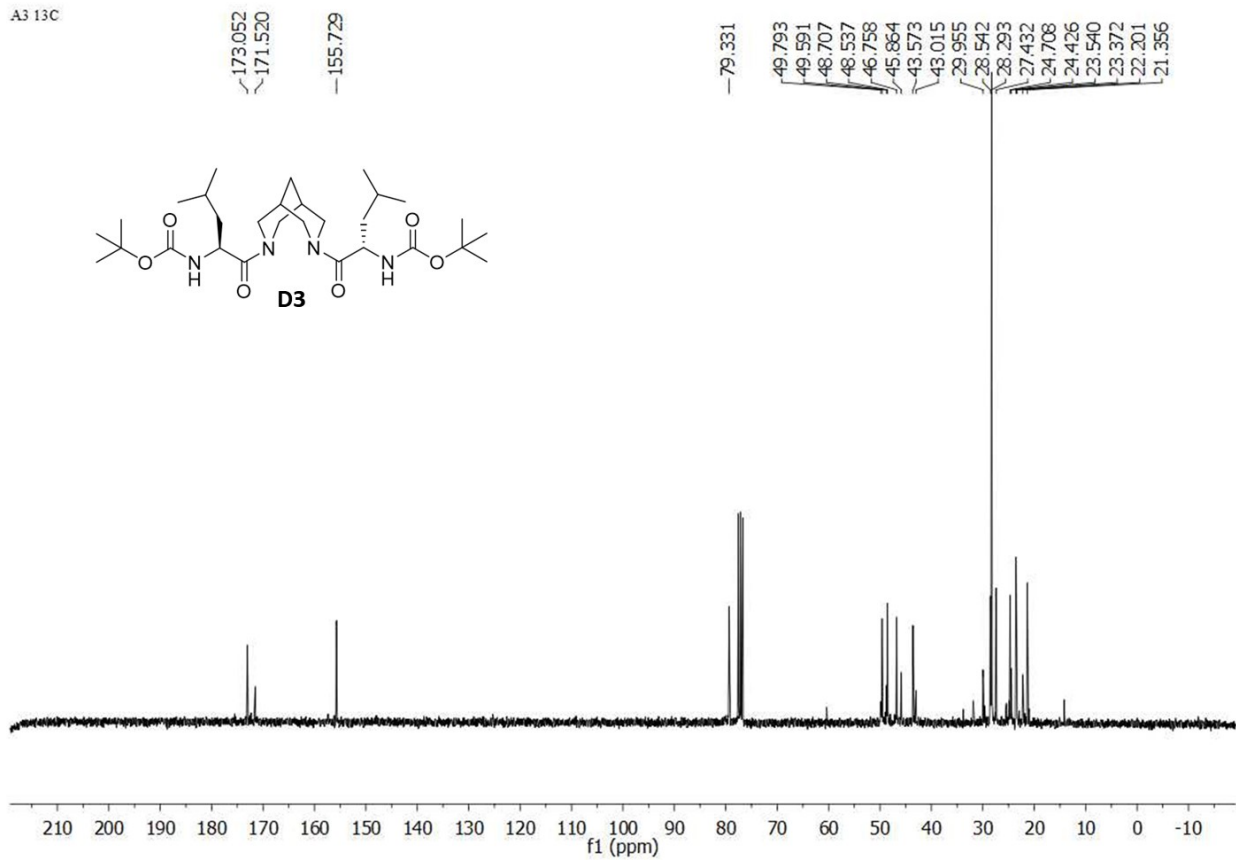
Meas. m/z	#	Ion Formula	m/z	err [ppm]	mSigma	# mSigma	Score	rdb	e ⁻ Conf	N-Rule
317.2200	1	C17H30N2NaO2	317.2199	-0.2	17.9	1	100.00	3.5	even	ok

HRMS of D2

A3 1H



A3 13C



^{13}C NMR (75 MHz, CDCl_3) of **D3**

Elemental Composition Report

Single Mass Analysis

Tolerance = 5.0 PPM / DBE: min = -1.5, max = 50.0

Element prediction: Off

Number of isotope peaks used for i-FIT = 3

Monoisotopic Mass, Even Electron Ions

1468 formula(e) evaluated with 9 results within limits (up to 10 best isotopic matches for each mass)

Elements Used:

C: 0-50 H: 0-60 N: 0-10 O: 0-12 Na: 0-1

XEVO -G2XSQTOF#TFC2176

POSITIVE ION MODE

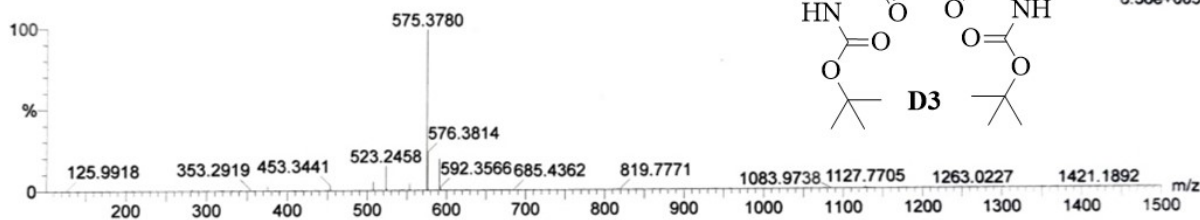
VH B (LBOC)2

01112022_2 29 (0.586)

Capillary V 3, Cone V 40, Desolvation Gas 800
ESI

01-Nov-2022

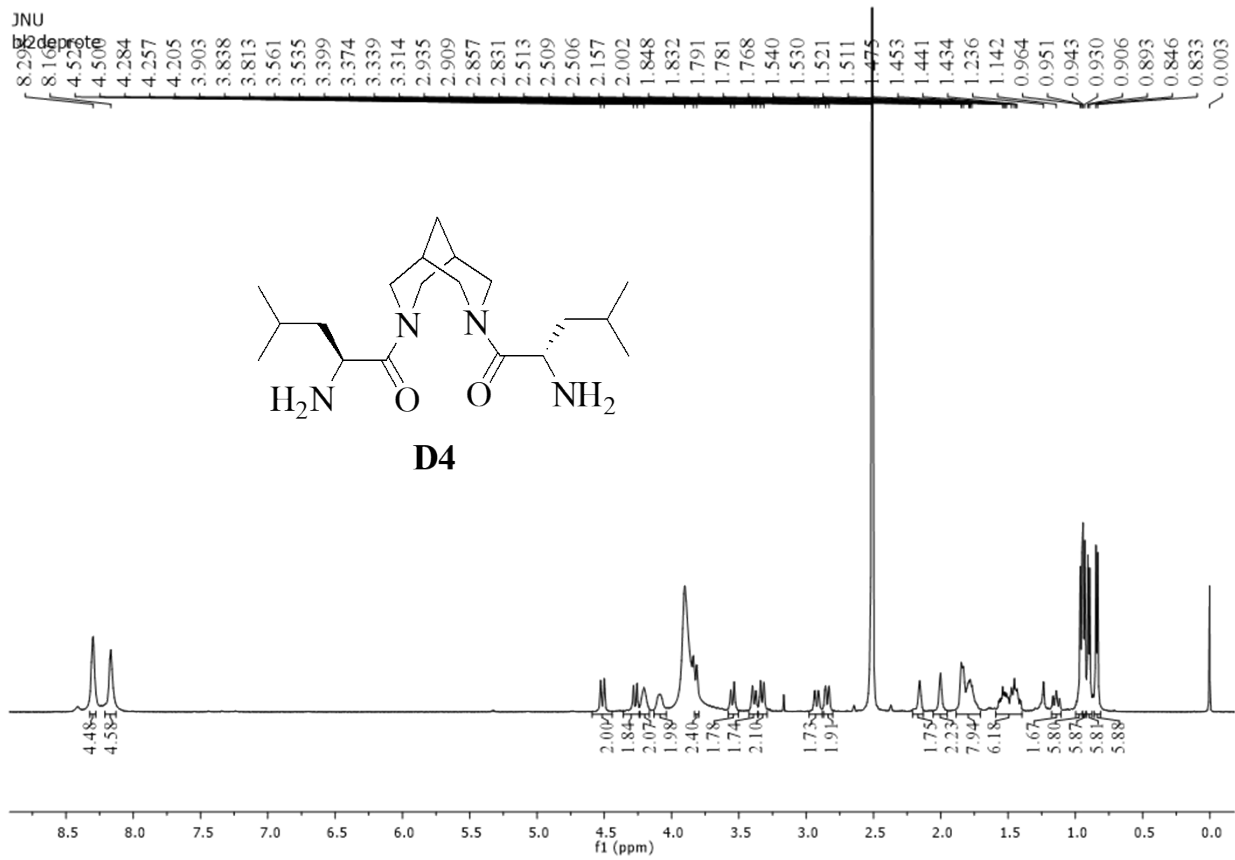
1: TOF MS ES+
6.36e+005



Minimum: -1.5
Maximum: 5.0 5.0 50.0

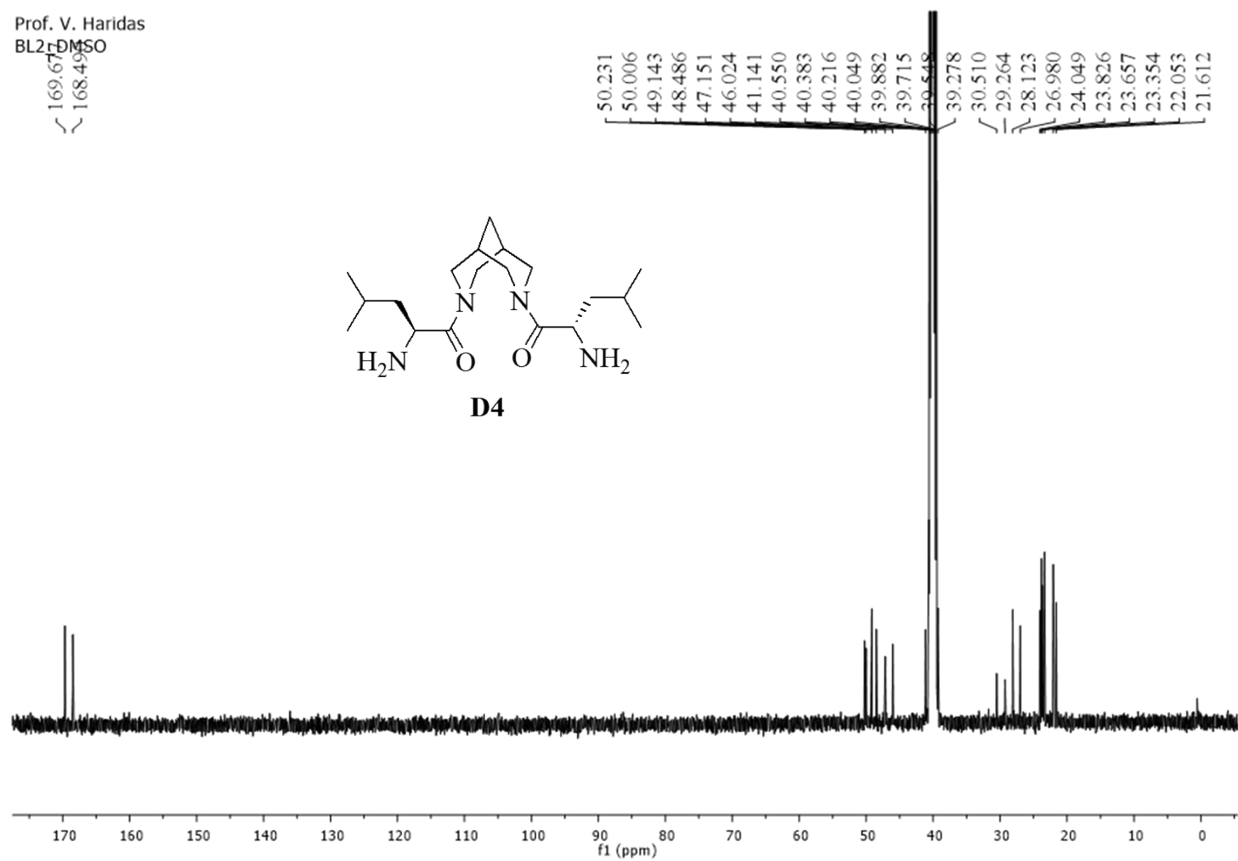
Mass	Calc. Mass	mDa	PPM	DBE	i-FIT	Norm	Conf (%)	Formula
575.3780	575.3785	-0.5	-0.9	5.5	49.9	1.887	15.16	C29 H52 N4 O6 Na
	575.3795	-1.5	-2.6	3.5	50.0	1.983	13.76	C30 H55 O10
	575.3798	-1.8	-3.1	10.5	50.0	2.006	13.45	C30 H48 N8 O2 Na
	575.3771	0.9	1.6	0.5	50.1	2.087	12.41	C28 H56 O10 Na
	575.3809	-2.9	-5.0	8.5	50.2	2.222	10.83	C31 H51 N4 O6
	575.3782	-0.2	-0.3	9.5	50.3	2.232	10.73	C27 H47 N10 O4
	575.3768	1.2	2.1	4.5	50.4	2.377	9.28	C26 H51 N6 O8
	575.3758	2.2	3.8	6.5	50.5	2.524	8.01	C25 H48 N10 O4 Na
	575.3755	2.5	4.3	-0.5	50.8	2.754	6.36	C25 H55 N2 O12

HRMS of D3



^1H NMR (500 MHz, $\text{DMSO-}d_6$) of **D4**

Prof. V. Haridas
BL2r-DMSO

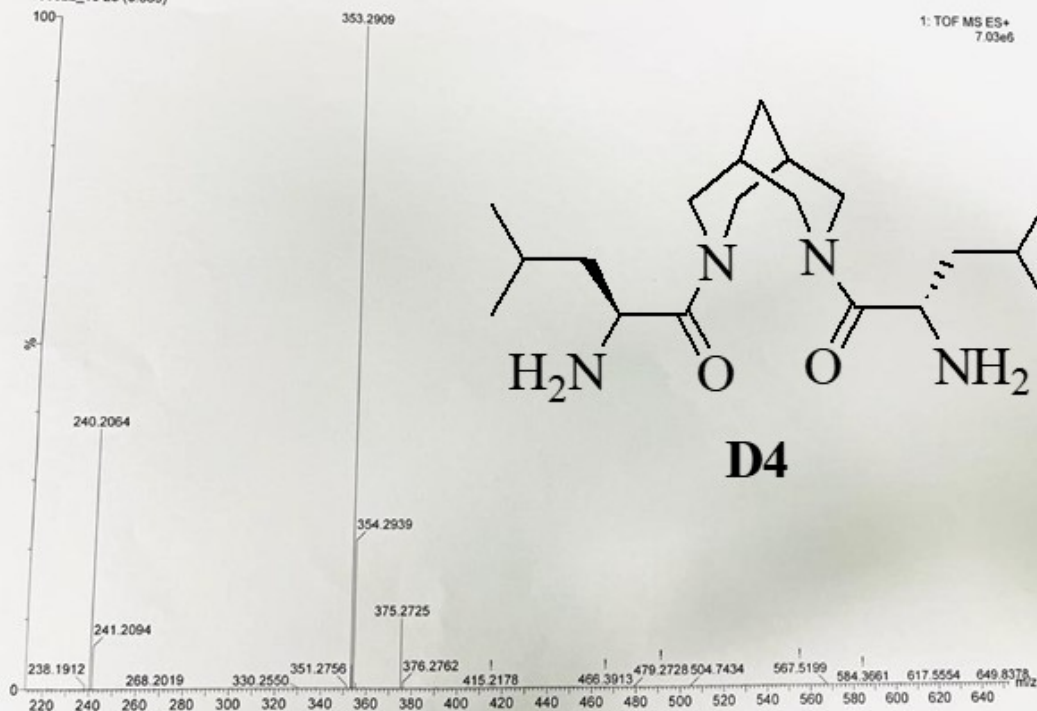


¹³C NMR (125 MHz, DMSO-*d*₆) of **D4**

XEVO-G2XSQTOF#YFC 2176
 POSITIVE ION MODE
 VH BL2
 180822_15 28 (0.569)

Capillary V 3, Cone V 40, Desolvation Gas 800,
 ESI

18-Aug-2022 15:06:32



Elemental Composition Report

Page 1

Single Mass Analysis

Tolerance = 5.0 PPM / DBE: min = -1.5, max = 50.0

Element prediction: Off

Number of isotope peaks used for i-FIT = 3

Monoisotopic Mass, Even Electron Ions

415 formula(e) evaluated with 2 results within limits (all results (up to 1000) for each mass)

Elements Used:

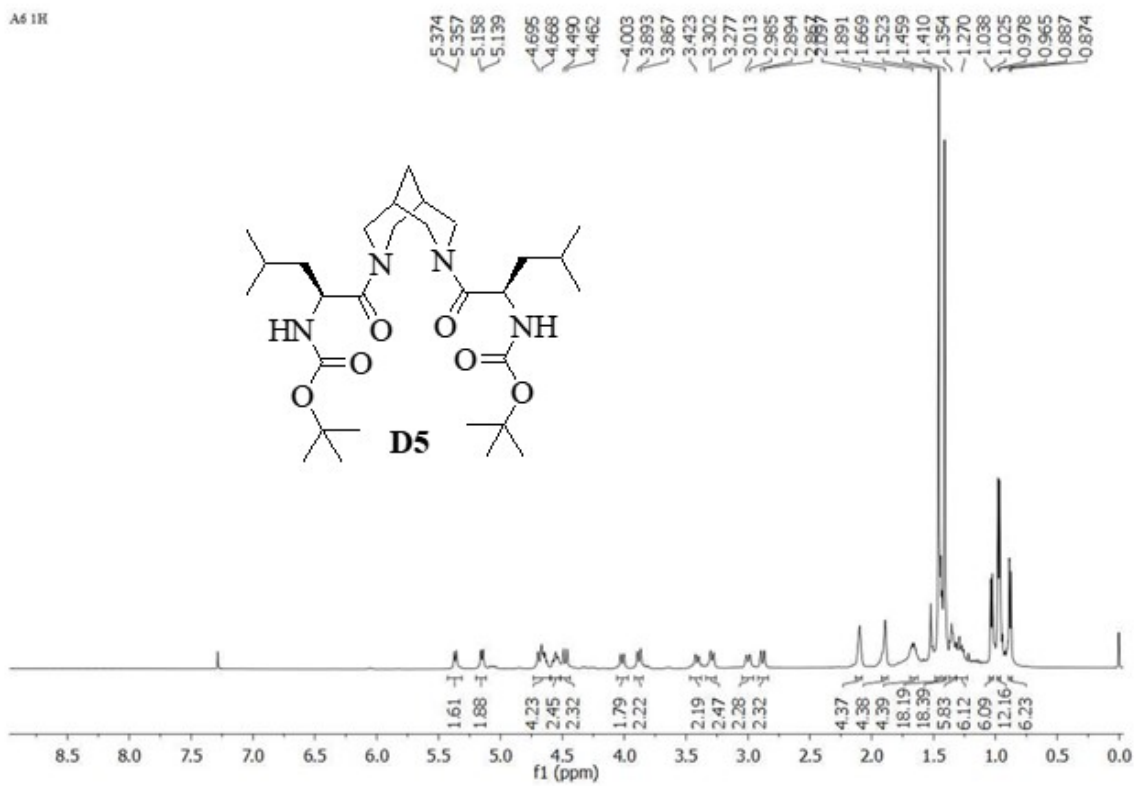
C: 0-50 H: 0-50 N: 0-5 O: 0-4 Na: 0-1 I: 0-1

Minimum:
 Maximum: 5.0 5.0 -1.5
 50.0

Mass	Calc. Mass	mDa	PPM	DBE	i-FIT	Norm	Conf (%)	Formula
353.2909	353.2917	-0.8	-2.3	3.5	180.6	0.155	85.61	C19 H37 N4 O2
	353.2892	1.7	4.8	0.5	182.4	1.939	14.39	C17 H38 N4 O2 Na

HRMS of D4

A6 1H



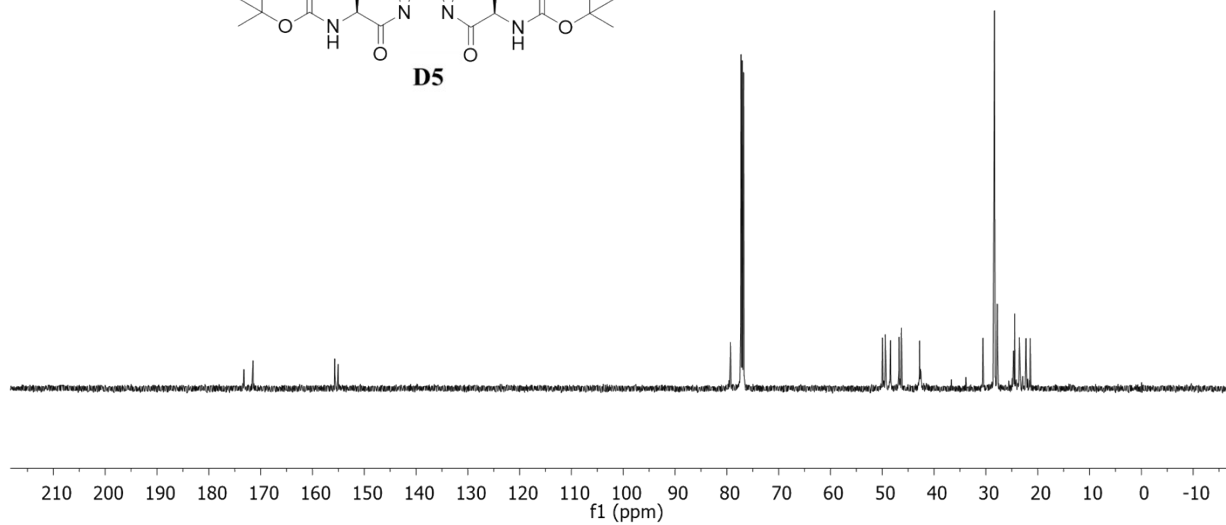
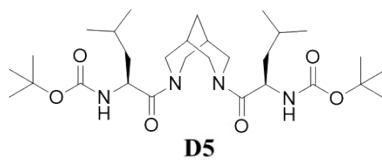
¹H NMR (500 MHz, CDCl₃) of **D5**

173.225
171.474

155.687
155.035

79.303
79.266

49.979
49.430
48.489
48.413
46.772
46.308
42.771
42.622
30.572
28.441
28.339
27.805
24.655
24.438
23.554
23.368
22.258
21.451



^{13}C NMR (125 MHz, CDCl_3) of **D5**

Elemental Composition Report

Single Mass Analysis

Tolerance = 5.0 PPM / DBE: min = -1.5, max = 50.0

Element prediction: Off

Number of isotope peaks used for i-FIT = 3

Monoisotopic Mass, Even Electron Ions

395 formula(e) evaluated with 2 results within limits (up to 10 best isotopic matches for each mass)

Elements Used:

C: 0-40 H: 0-60 N: 0-5 O: 0-7 Na: 0-1

XEVO -G2XSQTOF#TFC2176

Capillary V 3, Cone V 40, Desolvation Gas 800
ESI

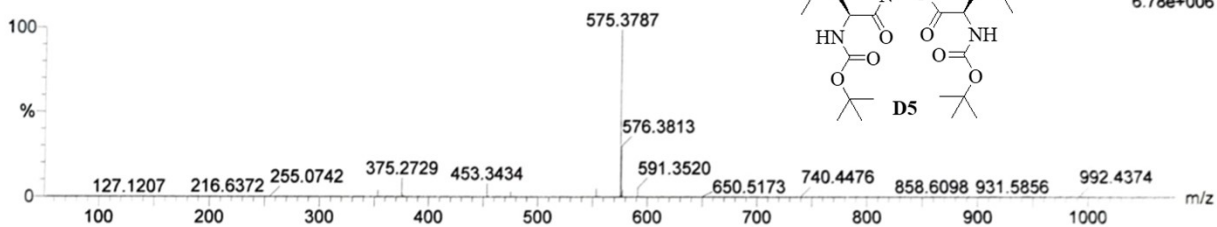
14-Oct-2022

POSITIVE ION MODE

VH BL2DL R

141022_7 17 (0.363)

1: TOF MS ES+
6.78e+006

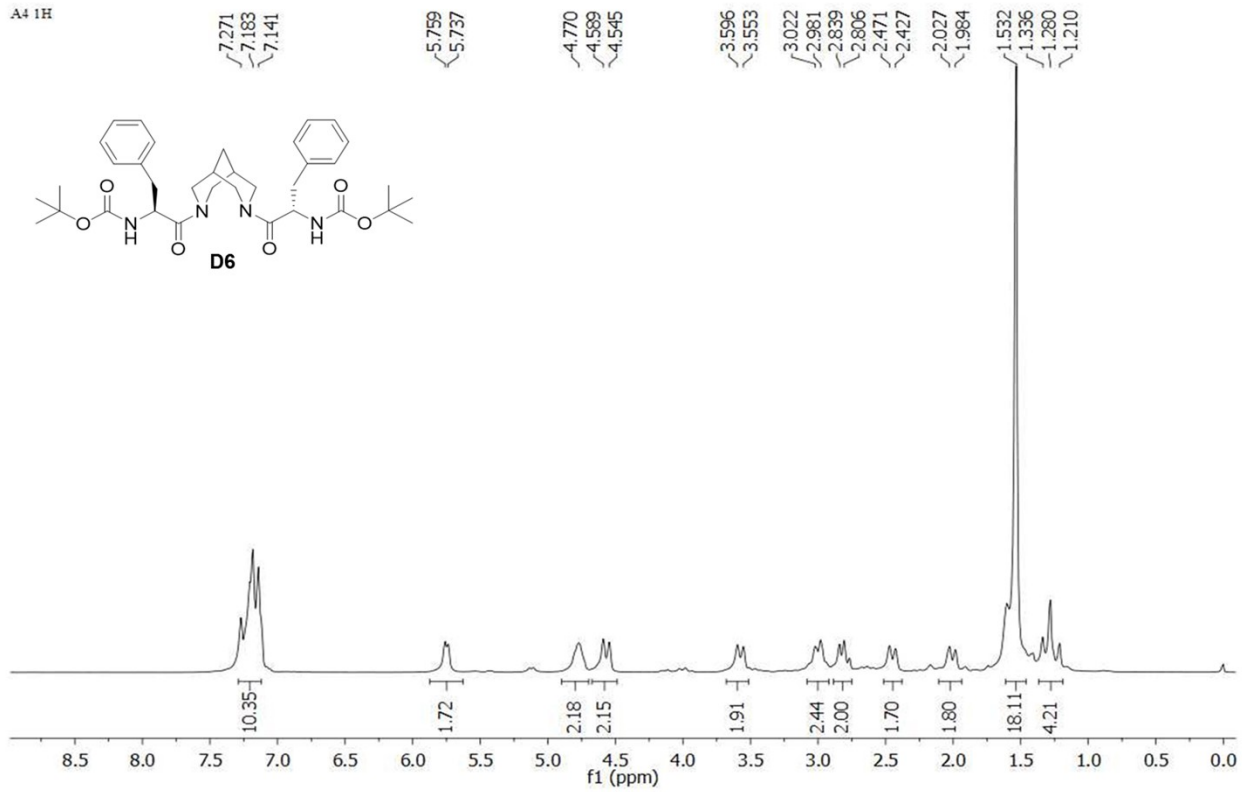


Minimum: -1.5
Maximum: 5.0 5.0 50.0

Mass	Calc. Mass	mDa	PPM	DBE	i-FIT	Norm	Conf(%)	Formula
575.3787	575.3785	0.2	0.3	5.5	142.1	0.024	97.66	C29 H52 N4 O6 Na
	575.3809	-2.2	-3.8	8.5	145.8	3.754	2.34	C31 H51 N4 O6

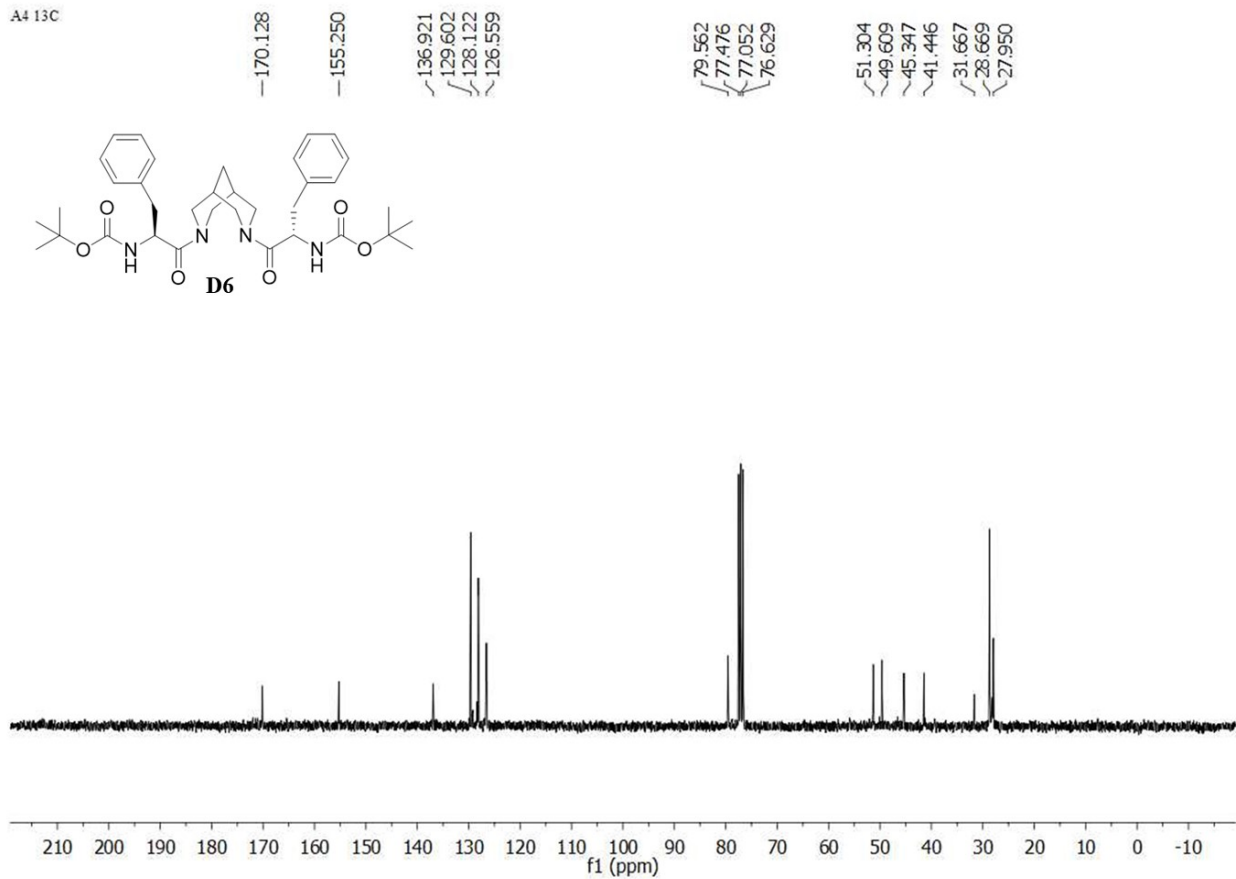
HRMS of D5

A4 1H



¹H NMR (300 MHz, CDCl₃) of **D6**

A4 13C



^{13}C NMR (75 MHz, CDCl_3) of **D6**

Mass Spectrum SmartFormula Report

Analysis Info

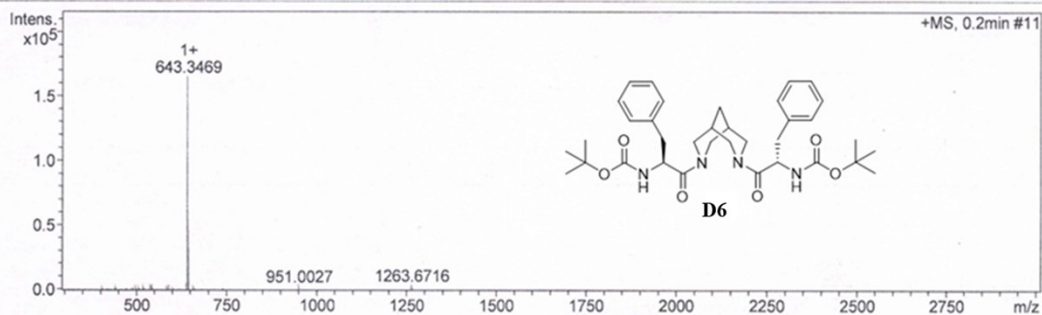
Analysis Name Y:\Data\DEC 2021\vh r 8000001.d
Method tune_wide.m
Sample Name tm 1 100
Comment

Acquisition Date 12/23/21 3:22:29 PM

Operator BDAL@DE
Instrument micrOTOF-Q 228888.10262

Acquisition Parameter

Source Type	ESI	Ion Polarity	Positive	Set Nebulizer	0.4 Bar
Focus	Active	Set Capillary	4500 V	Set Dry Heater	180 °C
Scan Begin	300 m/z	Set End Plate Offset	-500 V	Set Dry Gas	4.0 l/min
Scan End	3000 m/z	Set Collision Cell RF	700.0 Vpp	Set Divert Valve	Source



HRMS of D6

Reference

1. H. Singh, A. Chenna, U. Gangwar, J. Borah, G. Goel and V. Haridas, *Chem. Sci.*, 2021, **12**, 15757–15764.
2. F. Neese, *WIREs Comput Mol Sci*, , DOI:10.1002/wcms.1327.
3. The PyMOL Molecular Graphics System, Version 2.0 Schrödinger, LLC.
4. K. Vanommeslaeghe and A. D. MacKerell, *J. Chem. Inf. Model.*, 2012, **52**, 3144–3154.
5. M. J. Abraham, T. Murtola, R. Schulz, S. Páll, J. C. Smith, B. Hess and E. Lindahl, *SoftwareX*, 2015, **1–2**, 19–25.
6. J. Wang and B. L. Feringa, *Science*, 2011, **331**, 1429–1432.
7. P. A. Torrillo, A. T. Bogetti and L. T. Chong, *J. Phys. Chem. A*, 2021, **125**, 1642–1649.
8. G. A. Tribello, M. Bonomi, D. Branduardi, C. Camilloni and G. Bussi, *Computer Physics Communications*, 2014, **185**, 604–613.